

# Hot Radiative Accretion onto a Spinning Neutron Star

Mikhail V. Medvedev \*

Department of Physics and Astronomy,  
University of Kansas, KS 66045

March 20, 2022

## Abstract

A new type of self-similar hot viscous radiative accretion flow onto a rapidly spinning neutron star has recently been discovered. This “hot brake” flow forms in the two-temperature zone (close to a central object), but at a sufficiently low accretion rate and a high spin it may extend in the radial direction beyond  $\sim 300$  Schwarzschild radii into a one-temperature zone. When the spin of the star is small enough, the flow transforms smoothly to an advection-dominated accretion flow.

The properties of the hot brake flow are rather exceptional and surprising. All gas parameters (density, angular velocity, temperature, luminosity, angular momentum flux) except for the radial velocity are independent of the mass accretion rate; these quantities do depend sensitively on the spin of the neutron star. The gas angular momentum is transported outward under most conditions, hence the central star is nearly always spun-down. The luminosity of the hot brake flow arises from the rotational energy that is released as the star is braked by viscosity. The contribution from gravity is small, therefore the radiative efficiency may be arbitrarily large as  $\dot{M} \rightarrow 0$ . We demonstrate that the flow is also convectively stable and is unlikely to produce a strong outflow or wind.

---

\*Also at the Institute for Nuclear Fusion, RRC “Kurchatov Institute”, Moscow 123182, Russia

The hot brake flow is cooling-dominated (via Bremsstrahlung) and, hence, might be thermally unstable. The analysis of thermal conduction in the hot gas shows that thermal transport is collisionless (non-Spitzer) and occurs via free streaming of electrons along tangled magnetic field lines. We find that conduction is strong enough to make the flow thermally stable.

The very fact that the density, temperature and angular velocity of the gas at any radius in the hot brake flow are completely independent of the outer and inner (except for the star spin) boundary conditions implies that the flow cannot be smoothly matched to a general external medium as well as to general conditions on the star surface. We demonstrate that there are two extra self-similar solutions: one bridges the gap between the original solution and the external medium, and another represents a boundary layer between the bulk of the flow and the star surface, in which the gas temperature rapidly drops while the density builds up.

Finally, we briefly discuss that a hot brake flow may form around other rapidly spinning compact objects: white dwarfs and black holes.

## 1 Introduction

Accretion flows around compact objects frequently radiate significant levels of hard X-rays, indicating the presence of hot optically-thin gas in these systems. This has motivated the study of hot accretion flows around compact stars.

Zeldovich & Shakura (1969) and Alme & Wilson (1973) considered spherically free-falling plasma impinging on the surface of a neutron star (NS). They calculated the penetration depth of the falling protons and made preliminary estimates of the radiated spectrum. Their ideas were followed up by a number of later authors, e.g., Turolla et al. (1994), Zampieri et al. (1995), and Zane et al. (1998), who carried out more detailed computations of spectra.

A fluid approach to spherical accretion onto a NS was pioneered by Shapiro & Salpeter (1975), who worked out the structure of the standing shock in a spherical flow and computed the two-temperature structure of the post-shock gas and the resulting spectrum. The equivalent problem for an accreting white dwarf was analyzed by Kylafis & Lamb (1982). In related work, Chakrabarti & Sahu (1997) described the hydrodynamics of spherical

accretion onto black holes and NSs, but without including radiation processes.

All of the studies listed above involve inviscid spherical flows and include shocks of some kind, caused by spherically accreting matter crashing on the surface of the accreting star. However, if the accretion flow has angular momentum and viscous transport, there are strong reasons why a shock is not expected. A shock introduces a causal discontinuity between the accreting star and the inflowing gas. While such a discontinuity is not a problem for a spherical flow, Pringle (1977, see also Popham & Narayan 1992) argued that it leads to a serious physical inconsistency if the flow is rotating. Popham & Narayan (1992) showed that a causal viscosity prescription leads to consistent viscous accretion solutions without shocks. Popham & Sunyaev (2001) have calculated detailed boundary layer solutions for accretion onto a neutron star, but these solutions are based on the cool thin accretion disk model and are not relevant for the hot flows we discuss here.

One situation in which a shock is possible with a rotating flow is if the surface of the accreting star lies inside the marginally stable orbit of a thin disk. One then expects “gap accretion” with a shock (Kluźniak & Wilson 1991), and there is no inconsistency in having a shock. The marginally stable orbit appears not to play an important role in hot quasi-spherical flows (see Narayan, Kato, & Honma 1997 and Chen, Abramowicz & Lasota 1997). It is, therefore, not clear that one would necessarily have a shock with a hot flow even if the accreting star were very compact.

Deufel, Dullemond & Spruit (2001) modified the model of Zeldovich & Shakura (1969) by considering a rotating advection-dominated accretion flow (see below) around a NS. Their model represents an improvement on the earlier work since it includes angular momentum and viscosity, but it still invokes a shock of some kind, since there is a discontinuity at the radius where the hot ADAF meets the surface of the NS.

Following the seminal work on two-temperature accretion flows by Shapiro, Lightman, & Eardley (1976, the SLE solution), other hot solutions were discovered to describe accretion onto black holes: the advection-dominated accretion flow (ADAF) (Ichimaru 1977; Rees et al. 1982; Narayan & Yi 1994, 1995a,b; Abramowicz et al. 1995), the advection-dominated inflow-outflow solution (ADIOS) (Blandford & Begelman 1999; Narayan & Yi 1994, 1995a), and the convection-dominated accretion flow (CDAF) (Narayan et al. 2000; Quataert & Gruzinov 2000). All of these solutions describe rotating flows with viscosity and angular momentum transfer. The relevance of the solutions for accretion onto a NS is, however, un-

clear.

Recently, Medvedev & Narayan (2001a) discovered a rotating shock-free solution of the viscous fluid equations that corresponds to hot quasi-spherical accretion onto a rapidly spinning NS. We refer to this solution as a “*hot brake flow*,” since the gas is hot (the temperature is nearly virial) and it spins the NS down (in previous works it was called the “hot settling flow”). The solution could equally well be described as a “*hot atmosphere*” since the solution is to first approximation static, and accretion represents only a small perturbation on the static solution (as is probably true for any settling flow). To our knowledge, the hot brake flow is the only solution for accretion onto a NS presently available that does not involve a discontinuity near the surface of the star. The hot brake flow should not be confused with a boundary layer which forms in the very vicinity of the stellar surface (e.g., Narayan & Popham 1993) and which is characterized by a high gas density and steep spatial gradients of physical parameters. The hot brake flow forms *above* the boundary layer and extends radially to a large distance, typically thousands of stellar radii or more. Following up the work by (Davies & Pringle 1981), Ikhsanov (2001, 2003) has recently presented a subsonic hot accretion flow around a magnetized neutron star in the propeller state. The main difference between the two cases is that in the hot brake flow, heating and cooling balance each other, whereas in the subsonic propeller the heating rate of the accreting gas due to viscous dissipation is much larger than the radiative cooling rate. Hence, the latter solution shows some resemblance to the advection-dominated (or convection-dominated) flow.

The hot brake flow exists at rather low accretion rates, smaller than a few percent of Eddington. The flow is subsonic everywhere (which is why it does not form a shock near the NS surface). Because the accreting gas has a low density and high temperature, the particle mean free path is larger than the local radius of the flow and the gas is essentially collisionless. Viscosity plays a very important role; indeed, the flow is powered by the rotational energy of the central accretor which is braked by viscous torques. A very interesting property of the flow is that, except for the inflow velocity, all gas properties, such as density, temperature, angular velocity, luminosity, and angular momentum flux, are independent of the mass accretion rate, as might be expected from the earlier comment that accretion behaves like a minor perturbation on an intrinsically static solution; the flow properties do depend on the NS spin (see Medvedev & Narayan 2001a for more details).

In this paper we present the analytical self-similar solution describing

this *hot brake flow*, study its stability and observable properties. We also present the solution that matches the hot break flow to an arbitrary external medium and the boundary layer solution that matches the flow to the star surface. All our theoretical results are confirmed with numerical solutions of the appropriate set of hydrodynamic equations.

## 2 Basic considerations

### 2.1 The mathematical model

We consider gas accreting viscously onto a compact spinning object with a surface. The central object has a radius  $R_*$ , a mass  $M_* = mM_{\text{Sun}}$ , and an angular velocity  $\Omega_* = s\Omega_K(R_*)$ , where  $\Omega_K(R) = (GM_*/R^3)^{1/2}$  is the Keplerian angular velocity at radius  $R$ . We measure the accretion rate in Eddington units,  $\dot{m} = \dot{M}/\dot{M}_{\text{Edd}}$ , and the radius in Schwarzschild units,  $r = R/R_g$ , where  $\dot{M}_{\text{Edd}} = 1.39 \times 10^{18} m \text{ g s}^{-1}$  (corresponding to a radiative efficiency of 10%) and  $R_g = 2GM_*/c^2$ . We use the height-integrated form of the viscous hydrodynamic equations (Ichimaru 1977; Abramowicz, et al. 1988; Paczyński 1991; Narayan & Yi 1994):

$$\dot{M} = 4\pi R^2 \rho v, \quad (1)$$

$$v \frac{dv}{dR} = (\Omega^2 - \Omega_K^2) R - \frac{1}{\rho} \frac{d}{dR} (\rho c_s^2), \quad (2)$$

$$4\pi\nu\rho R^4 \frac{d\Omega}{dR} = \dot{J} - \dot{M}\Omega R^2, \quad (3)$$

$$\rho v T_p \frac{ds_p}{dR} = \frac{\rho v c^2}{(\gamma_p - 1)} \frac{d\theta_p}{dR} - v c^2 \theta_p \frac{d\rho}{dR} = q^+ - q_{\text{Coul}}, \quad (4)$$

$$\rho_e v T_e \frac{ds_e}{dR} = \frac{\rho_e v c^2}{(\gamma_e - 1)} \frac{d\theta_e}{dR} - v c^2 \theta_e \frac{d\rho_e}{dR} = q_{\text{Coul}} - q^-, \quad (5)$$

where  $\rho$  is the mass density of the accreting gas,  $v$  is the radial infall velocity,  $\Omega$  is the angular velocity,  $c_s^2 = c^2(\theta_p + \theta_e m_e/m_p)$  is the square of the isothermal sound speed,  $T_{p,e}$  are the temperatures of protons and electrons,  $\theta_{p,e} = k_B T_{p,e}/m_{p,e} c^2$  are the corresponding dimensionless temperatures,  $\nu$  is the gas viscosity,  $\dot{J}$  is the rate of accretion of angular momentum,  $s_p$  and  $s_e$  are the specific entropies of the proton and electron fluids,  $\rho_e \simeq (m_e/m_p)\rho$  is the mass density of the electron fluid,  $\gamma_p$  and  $\gamma_e$  are the adiabatic indexes of

protons and electrons (which, in general, may be functions of  $T_p$  and  $T_e$ ), and  $q^+$ ,  $q^-$ , and  $q_{\text{Coul}}$  are the viscous heating rate, radiative cooling rate, and energy transfer rate from protons to electrons via Coulomb collisions, per unit mass. We have assumed that all viscous heat goes into the proton component. Equations (1)–(5) describe the conservation of mass, radial momentum, angular momentum, proton energy and electron energy, respectively.

We employ the usual  $\alpha$  prescription for the kinematic coefficient of viscosity, which we write as

$$\nu = \alpha c_s H \approx \alpha c_s R. \quad (6)$$

Often, in accretion problems, one makes use of the relation  $H = c_s/\Omega_K$  and writes  $\nu = \alpha c_s^2/\Omega_K$ . This prescription is equivalent to  $\nu = \alpha c_s H \approx \alpha c_s R$  in the regime of the Medvedev & Narayan (2001a) hot brake flow. However, in the outer regions of the flow, where the other solutions described in the following sections appear,  $H$  is much less than  $c_s/\Omega_K$ , and  $\nu = \alpha c_s^2/\Omega_K$  is not a good approximation. Equation (6) is a superior prescription and is physically better motivated over a wide range of conditions (so long as the flow is quasi-spherical).

We assumed that the flow is hot and quasi-spherical, which generally requires a low mass accretion rate (see Narayan, et al. 1997). The accreting gas has nearly the virial temperature, i.e.,  $c_s^2 \sim GM_*/R \sim (\Omega_K R)^2$ , and the local vertical scale height  $H = c_s/\Omega_K$  is comparable to the local radius  $R$ . We may then use the height integrated hydrodynamic equations for a steady, rotating, axisymmetric flow, and for simplicity we may set  $H = R$  (Medvedev & Narayan 2001a).

In the case of accretion onto a NS we expect the flow to slow down as it settles on the stellar surface, and we expect the density in this settling zone to be significantly higher than for a black hole (BH) accretion. The increased density would cause more efficient transfer of energy from protons to electrons via Coulomb collisions and more efficient radiation from the electrons. As we show below, this leads to a flow in which  $q^+$ ,  $q^-$  and  $q_{\text{Coul}}$  are all of the same order, which is very different from the case of a BH ADAF, where  $q^+ \gg q^-$ ,  $q_{\text{Coul}}$ . Another feature of the settling zone, again the result of the large density, is that optically thin bremsstrahlung cooling (which is sensitive to  $\rho$ ) dominates over self-absorbed synchrotron cooling. We therefore neglect synchrotron emission in our analysis. For simplicity, we neglect also thermal conduction (we will include this effect in the discussion of thermal stability).

The temperature of the gas determines the efficiency of the Coulomb energy transfer from the protons to the electrons and the rate of Bremsstrahlung cooling of the electrons. The balance between them defines whether the gas is in the two temperature regime (when the temperatures are high and the Coulomb collisions are very rare) or in the one-temperature regime (then temperatures are lower).

The two-temperature regime occurs closer to the central object, where the virial temperature high enough and the electrons become relativistic. In the inner region of the flow,  $R_* \lesssim R \lesssim 100R_*$ . we expect a two-temperature plasma, with  $T_p > T_e$ , in which the electrons are relativistic and the protons are non-relativistic:  $\theta_e \gg 1$ ,  $\theta_p \ll 1$ . The viscous heating rate of the gas, the energy transfer rate from the protons to the electrons via Coulomb collisions, and the cooling rate of the electrons via bremsstrahlung emission are given by

$$q^+ = \nu \rho R^2 \left( \frac{d\Omega}{dR} \right)^2, \quad (7)$$

$$q_{\text{Coul}} = Q_{\text{Coul}} \rho^2 \frac{\theta_p}{\theta_e}, \quad Q_{\text{Coul}} = 4\pi r_e^2 \ln \Lambda \frac{m_e c^3}{m_p^2}, \quad (8)$$

$$q^- = Q_{\text{ff,R}} \rho^2 \theta_e, \quad Q_{\text{ff,R}} = 48\alpha_f r_e^2 \frac{m_e c^3}{m_p^2}, \quad (9)$$

where  $\alpha_f$  is the fine structure constant,  $r_e$  is the classical electron radius,  $\ln \Lambda \simeq 20$  is the Coulomb logarithm,  $c_s^2 \simeq c^2 \theta_p$ , and we have neglected logarithmic corrections to the relativistic free-free emissivity. The subscript “R” in  $Q_{\text{ff,R}}$  denotes relativistic Bremsstrahlung.

For  $R > 100R_*$ , both protons and electrons are non-relativistic and have nearly the same temperature  $T_p - T_e \ll T_p, T_e$ . The free-free cooling takes the form

$$q^- = Q_{\text{ff,NR}} \rho^2 \theta_e^{1/2}, \quad Q_{\text{ff,NR}} = 5\sqrt{2}\pi^{-3/2} \alpha_f \sigma_T \frac{m_e c^3}{m_p^2}, \quad (10)$$

where  $\sigma_T$  is the Thompson cross-section, and the subscript NR stands for non-relativistic. Since the gas is effectively one-temperature, we have

$$q^+ \simeq q^- \quad (11)$$

because the Coulomb transfer rate,  $q_{\text{Coul}}$ , is proportional to  $(T_p - T_e)$  and can adjust itself to have the right magnitude with small adjustments of the two

temperatures. In the non-relativistic regime,  $\theta_e < 1$ ,  $\theta_p \sim (m_e/m_p)\theta_e \ll 1$ , and the Coulomb transfer rate is

$$q_{\text{Coul}} = \frac{3}{\sqrt{2\pi}} \frac{m_e}{m_p} \frac{\sigma_{TC}}{m_p^2} \ln \Lambda \rho^2 \frac{kT_p - kT_e}{\theta_e^{3/2} e^{-1/\theta_e}}. \quad (12)$$

From the condition  $q_{\text{Coul}} \simeq q^-$  it follows that

$$kT_p - kT_e \simeq \frac{10}{3\pi^2} \frac{\alpha_f}{\ln \Lambda} \sqrt{m_p m_e} c^2 \theta_e^2 e^{-1/\theta_e}, \quad (13)$$

which is exponentially small for  $\theta_e < 1$ .

The set of equations (1)–(5) must satisfy certain boundary conditions at the neutron star. First, as the flow approaches the surface of the star at  $R = R_*$ , the radial velocity must become very much smaller than the local free-fall velocity. Second, the angular velocity must approach the angular velocity of the star  $\Omega_*$ .

The radius of the star, and its spin, are the two principal boundary conditions applied at the inner edge of the accretion flow. We assume that the star is unmagnetized, so there are no magnetospheric effects to consider. Two outer boundary conditions, namely the temperature and angular velocity of the gas, are determined by the properties of the gas as it is introduced into the accretion flow on the outside (we will discuss this in subsequent sections). An additional important boundary condition is the mass accretion rate  $\dot{M}$ , which is determined by external conditions and which we take to be constant.

## 2.2 Numerical solution

The system of equations given above with appropriate boundary conditions has been solved using the relaxation method on a highly non-uniform grid (in order to resolve the thin boundary layer, where the density rises by few orders of magnitude).

We employ the gravitational potential of Paczyński & Wiita (1980) to mimic the effect of strong gravity near the NS surface. In this potential the Keplerian angular velocity takes the form

$$\Omega_K^2 = \frac{GM_*}{(R - R_g)^2 R}. \quad (14)$$

Note that the analytical work presented in the following sections is based on a Newtonian potential.



We specify the boundary conditions as follows. We take the outer boundary of the flow to be at  $R_{\text{out}} = 10^6 R_g$ . At this radius we specify that the angular velocity is equal to its value in the self-similar ADAF solution of Narayan & Yi (1994), and that the proton and electron temperatures are both equal to the self-similar ADAF temperature. We assume that the accreting star is a  $1M_{\text{Sun}}$  neutron star with a radius  $R_* = 3R_g = 8.85$  km, unless stated otherwise. At  $R = R_*$ , we specify the value of the NS spin parameter,  $s = \Omega_*/\Omega_K(R_*)$ , and we require the proton temperature of the flow to be  $T = \text{few} \times 10^7$  K  $\ll T_{\text{virial}}$ . (We do not assume that the electron and proton temperatures are equal, but in fact they are equal.) We do not constrain the density of the gas in any way at either boundary.

The numerical problem as posed here has a family of solutions characterized by three dimensionless parameters: the mass accretion rate  $\dot{m}$  (in Eddington units), the NS spin  $s$  (in units of the Keplerian angular velocity at the NS surface), and the viscosity parameter  $\alpha$ . The angular momentum flux  $\dot{J}$ , or equivalently the dimensionless flux  $j = \dot{J}/\dot{M}\Omega_K(R_*)R_*^2$ , is an eigenvalue of the problem.

It is known that a hot flow with low  $\dot{m}$  around a black hole is an “advection-dominated” accretion flow (ADAF). It has a two-temperature structure for  $R \lesssim 300R_g$  and is very hot (nearly virial) for all  $R$ . This solution has indeed been obtained numerically for  $\dot{m} \lesssim 0.01$  and  $s \lesssim 0.01$ . An interesting feature of the  $s = 0.01$  ADAF-type solution is that it consists of two distinct segments. For large radii (beyond  $R \sim 20R_g$  in Fig. 1), the flow corresponds to the standard ADAF discussed in the literature, with the scalings

$$\rho \propto r^{-3/2}, \quad c_s^2 \propto r^{-1}, \quad \Omega \propto r^{-3/2}, \quad v \propto r^{-1/2}. \quad (15)$$

However, at smaller radii, the numerical solution indicates the presence of a second advection-dominated zone, a “settling ADAF,” which was first seen in numerical calculations described in Narayan & Yi (1994). This settling ADAF is seen in Fig. 1 as a zone that lies between the boundary layer region and the outer standard ADAF, with different slopes for  $\rho$  and  $v$ . The radial extent of the settling ADAF zone may be quite large and, in general, depends on the flow parameters and boundary conditions.

A self-similar model of the settling ADAF may be readily obtained as follows. In an ADAF, energy is not radiated, therefore  $q^- = 0$ . Close to the star  $\Omega \simeq \text{constant}$ , therefore  $q^+ = 0$ . Equations (4), (5) then simplify to the condition of entropy conservation,  $ds/dR = 0$ , which yields  $c_s^2 \propto \rho^{\gamma-1}$ .

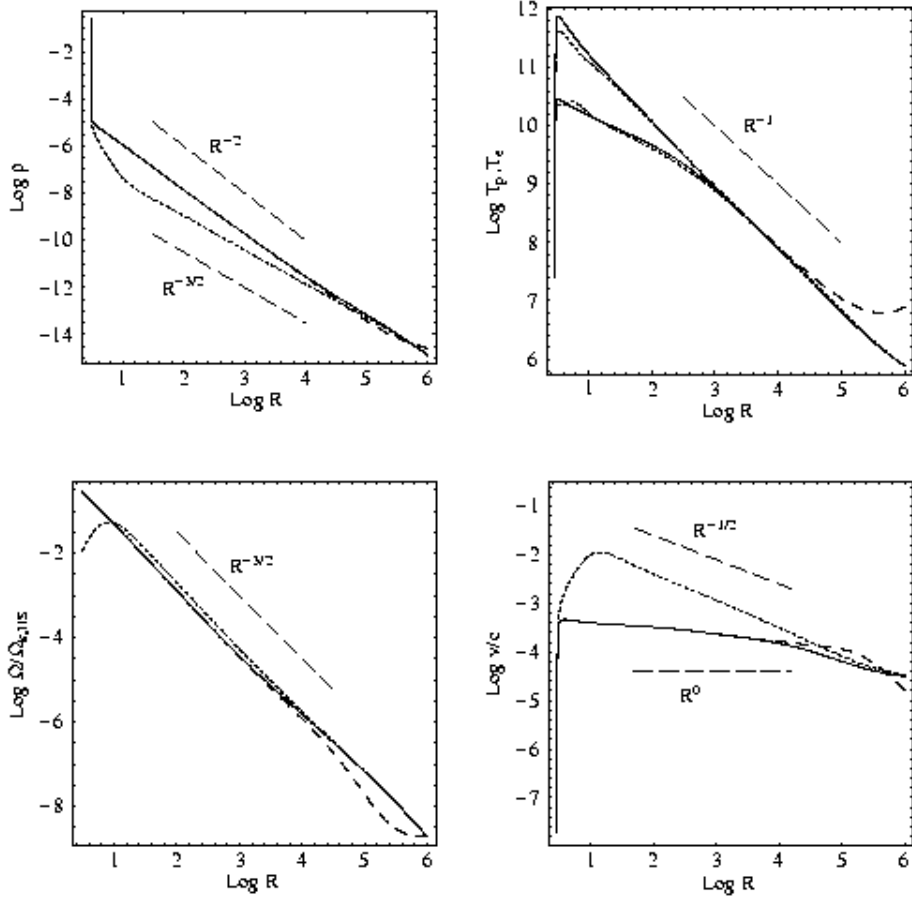


Figure 1: Profiles of density  $\rho$  ( $\text{g cm}^{-3}$ ), proton temperature  $T_p$  ( $^{\circ}\text{K}$ ), electron temperature  $T_e$  ( $^{\circ}\text{K}$ ), angular velocity  $\Omega$  (in units of the Keplerian angular velocity at the NS radius  $R_*$ ), and radial velocity  $v$  (in units of  $c$ ) for accretion flows with  $\alpha = 0.1$ ,  $\dot{m} = 0.01$ ,  $\gamma = 4/3$  and  $s = 0.3$  (solid curve) and  $s = 0.01$  (dotted curve). The self-similar slopes for an ADAF flow and a settling flow are shown for comparison. The long-dashed curves represent the same solution as the solid curve, but with ten times higher temperature at  $R_{out}$ .

As the material settles on the star, its radial velocity decreases and we have  $v \ll v_{ff}$ ,  $\Omega \ll \Omega_K$ . Then, from equation (2), it follows that the temperature of the gas is nearly virial. Other quantities are determined straightforwardly, so that we have

$$\rho \propto r^{\frac{1}{\gamma-1}}, \quad c_s^2 \propto r^{-1}, \quad \Omega \sim \text{const.}, \quad v \propto r^{-\frac{2\gamma-3}{\gamma-1}}. \quad (16)$$

The infall velocity decreases with radius if  $\gamma < 1.5$ , and increases if  $\gamma > 1.5$ . To highlight the difference between the standard ADAF and the settling ADAF, we have chosen  $\gamma = 4/3$  in the solutions shown in Fig. 1.

## 3 Hot brake flow

### 3.1 Numerical discovery

By solving the equations numerically for different values of  $s$ , we have found that the with increasing  $s$  the ADAF solution continuously transforms into a solution of another type. For relatively rapidly rotating stars, with  $s \gtrsim 0.1$ , the new *hot break* solution (which was referred in the previous works as the *settling solution*) is already well-established. The transition is not sharp, so it is difficult to identify a specific transition point  $s = s_t$  at which the transformation occurs. Numerical experiments indicate that the value of  $s_t$  (however it is defined) is not very sensitive to  $R_{out}$ ,  $\gamma$ , and  $\dot{m}$  and is, roughly,  $s_t \sim 0.04 - 0.06$ .

The change of the nature of the flow as  $s$  is varied is illustrated in Fig. 1. The solid and dotted curves correspond to two solutions with  $s = 0.3$  and  $s = 0.01$ , respectively, with all other boundary conditions being the same. We see that the solutions are markedly different from each other. This is most clearly seen in the profiles of density, where the  $s = 0.3$  model has a logarithmic slope of  $-2$ , as appropriate for the cooling-dominated settling solution described in this paper, and the  $s = 0.01$  model has a slope of  $-3/2$ , as expected for a standard self-similar ADAF (Narayan & Yi 1994, 1995a). There is a similar difference also in the profiles of the radial velocity, where the two solutions have logarithmic slopes of  $-1/2$  and  $0$ , respectively.

Figure 2 shows representative solutions for  $\alpha = 0.1$  and a range of values of  $\dot{m}$  and  $s$ . The solutions clearly have three radial zones. For  $R > 300R_g$ , there is a one-temperature zone in which the gas properties vary roughly as power-laws of the radius. For  $R < 300R_g$ , there is a second power-law

zone with a two-temperature structure. Finally, close to the NS, the flow has a boundary layer region. In this final region, the gas experiences runaway cooling, the velocity falls precipitously, and the density increases very rapidly.

The solutions are suspect also in the inner region of the two-temperature power-law zone and in the boundary layer, where Comptonization is likely to be important. Outside these regions, however, the numerical solution is expected to be accurate.

We note here some qualitative results: (i) the boundary layer always forms near the star surface, (ii) the transition radius where the boundary layer meets the outer settling flow is usually at  $R_{tr} \sim R_*$ , (iii) the value of  $R_{tr}$  depends on the NS spin. These results are in agreement with the studies by Titarchuk, Lapidus & Muslimov (1998) and Titarchuk & Osherovich (1999), and are important for the interpretation of kHz quasi-periodic oscillations.

An interesting property of the new solution is its insensitivity to the value of accretion rate (provided it is low enough). In our numerical solutions, curves corresponding to a given value of  $s$  and different values of  $\dot{m}$  coincide with one other to very good accuracy. This is best seen in the profiles of  $\rho$  and  $\Omega$ . Changing  $s$  causes an up/down shift of the curves but does not affect the slopes of the curves. The temperature profiles are sensitive to the spin  $s$ , especially for large values of  $s$ . The radial velocity varies approximately as  $v \propto \dot{m}$  and is roughly consistent with  $v \propto r^0$  for  $s > 0.1$ .

## 3.2 Self-similar solution

We now find the hot break solution analytically. The hot brake flow forms at low mass accretion rates. Therefore, for simplicity, we set  $\dot{m} = 0$  and omit the continuity equation. Thus, the gas configuration corresponds to a radially static “atmosphere.” The motivation for this approximation follows from the observation that the density  $\rho$ , temperature  $T$  and the angular velocity  $\Omega$  of the gas in the Medvedev & Narayan (2001a) self-similar solution are completely independent of  $\dot{m}$ . Only the radial velocity  $v$  depends on  $\dot{m}$ , and it is given trivially by the spherical continuity equation

$$v = \frac{\dot{M}}{4\pi R^2 \rho}. \quad (17)$$

Because of this, we do not lose any generality by setting  $\dot{m} = v = 0$  in the analysis; we may always introduce a finite  $\dot{m}$  and finite  $v$  after the fact.

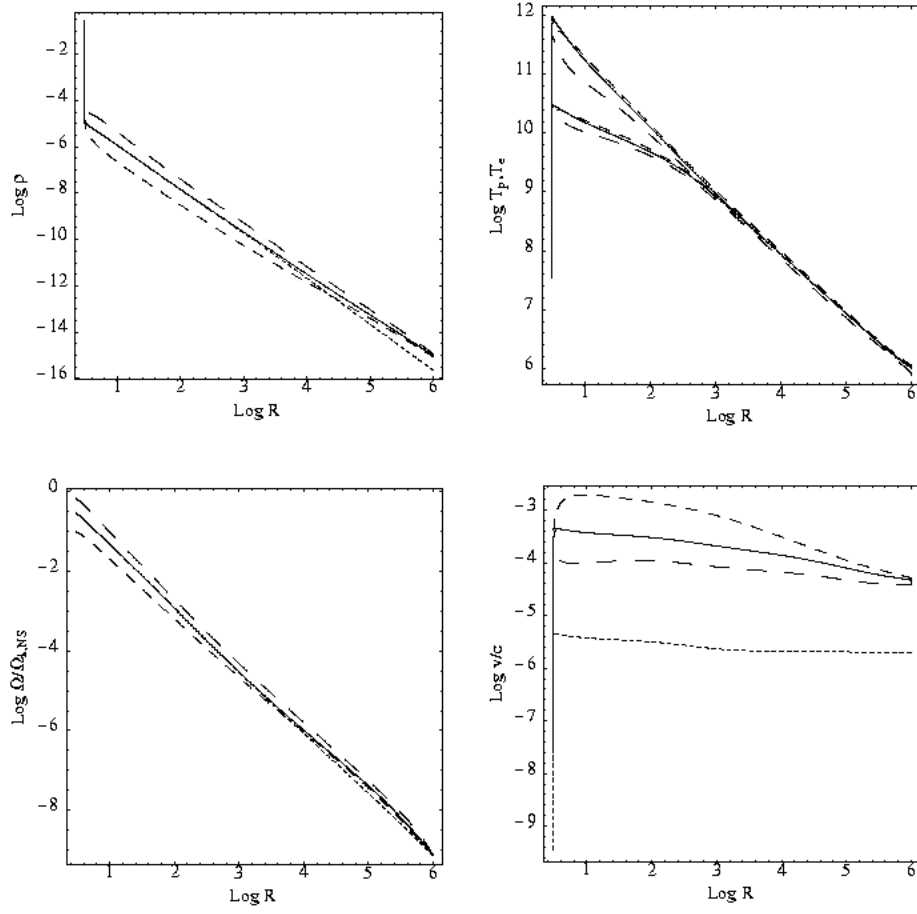


Figure 2: Profiles of density  $\rho$  ( $\text{g cm}^{-3}$ ), proton temperature  $T_p$  ( $^{\circ}\text{K}$ ), electron temperature  $T_e$  ( $^{\circ}\text{K}$ ), angular velocity  $\Omega$  (in units of the Keplerian angular velocity at the NS radius  $R_{NS}$ ), and radial velocity  $v$  (in units of  $c$ ) for accretion flows with  $\alpha = 0.1$  and  $(\dot{m}, s) = (0.01, 0.3)$  – solid line,  $(0.0001, 0.3)$  – short-dashed line,  $(0.01, 0.1)$  – medium-dashed line,  $(0.01, 0.7)$  – long-dashed line.

When  $v \neq 0$ , the energy equation has an extra term corresponding to the advection of energy. In advection-dominated accretion flows, for instance, this term dominates over the cooling term  $q^-$  (Narayan, et al. 1997). In the present case, however, we consider a situation in which the advection term is negligible (which corresponds to low  $\dot{m}$ ).

We assume that the flow is highly sub-Keplerian,  $\Omega(R) \ll \Omega_K(R)$ , so that the centrifugal support is negligible compared to the pressure support. The radial momentum equation then takes the following simple form,

$$\frac{GM_*}{R^2} = -\frac{1}{\rho} \frac{d(\rho c_s^2)}{dR}, \quad (18)$$

where we have used the fact that  $v \sim 0$  and written the pressure as  $p = \rho c_s^2$  where  $c_s$  is the isothermal sound speed. Medvedev & Narayan (2001a) present a more complete analysis in which they do not assume that the rotation is slow. They then obtain an extra factor of  $(1-s^2)$  in their equation, which propagates through to all the results. Since we ignore the factor, our analysis corresponds to the case of a slowly-spinning star:  $s^2 \ll 1$ . This approximation is made only to simplify the analysis, and all the results may be generalized for arbitrary  $s$ .

From the analysis by Medvedev & Narayan (2001a), we know that the accreting gas in our problem acts as a brake on the central spinning star and transports angular momentum outward through the action of viscosity. We therefore write the angular momentum conservation equation for the gas as follows,

$$\dot{J} = 4\pi\nu\rho R^4 \frac{d\Omega}{dR} = \text{constant}, \quad (19)$$

where  $\dot{J}$  is the outward angular momentum flux, and  $\nu$  is the kinematic coefficient of viscosity. This equation is exactly valid in steady state if  $\dot{m} = 0$ . When  $\dot{m}$  is non-zero, there is an additional term,  $\dot{M}\Omega R^2$ , due to the flux of angular momentum carried in by the accreting gas. The key feature of the hot brake solution is that the latter flux is negligible compared to the outward flux from the star. Equation (19) is, therefore, valid even when  $\dot{m} \neq 0$ , so long as  $\dot{m}$  is small enough for the term  $\dot{M}\Omega R^2$  to be negligible.

We first consider the *one-temperature* regime. The energy equations for the electrons and protons reduce in this case to

$$q^+ \simeq q^-. \quad (20)$$

The self-similar solution for the hot brake flow is then straightforwardly obtained. The gas parameters have the following radial dependences:

$$\rho = \rho_1 r^{-2}, \quad T = T_1 r^{-1}, \quad \Omega = \Omega_1 r^{-3/2}. \quad (21)$$

The subscript “1” in the coefficients is to indicate that this is the first (hot brake) solution, to distinguish it from other solutions described later. By substituting the above solution in equations (18), (19) and (20), we see that it satisfies the basic conservation laws. We may also solve for the numerical constants:

$$\rho_1 = \frac{\alpha s^2}{R_g} \frac{9}{2^{5/2}} \left( \frac{m_e}{m_p} \right)^{1/2} c^3 Q_{\text{ff,NR}}, \quad (22)$$

$$kT_1 = \frac{m_p c^2}{12}, \quad (23)$$

$$\Omega_1 = \frac{s c}{\sqrt{2} R_g} = s \Omega_K(R_g). \quad (24)$$

We note that if  $\dot{m} \neq 0$  then the flow has a small constant radial velocity:

$$v \propto r^0, \quad (25)$$

as follows from equation (17).

The angular momentum flux in the solution is given by

$$\dot{J} = -\alpha^2 s^3 R_g^2 \frac{3^{5/2}}{2^{5/2}} \left( \frac{m_e}{m_p} \right)^{1/2} \frac{c^5}{Q_{\text{ff,NR}}}. \quad (26)$$

By assumption, this flux is much greater than the angular momentum flux due to accretion, which sets an upper limit on the mass accretion rate for the solution to be valid (Medvedev & Narayan 2001a).

The pressure in the flow is given by

$$p = \rho c_s^2 = \rho_1 c_{s1}^2 r^{-3} \equiv p_1 r^{-3}, \quad (27)$$

where  $c_{s1}^2 = 2kT_1/m_p$ . If the accretion flow is immersed into an interstellar medium with some external gas pressure  $p_{\text{ext}}$ , then the above self-similar solution describes the flow at radii  $r \ll (p_1/p_{\text{ext}})^{1/3}$ , where the pressure  $p \gg p_{\text{ext}}$ .

This solution can be generalized to the *two-temperature* regime. In this case the electrons and proton energies are governed by two separate equations, which under our assumptions reduce to

$$q^+ = q_{\text{Coul}} \quad \text{and} \quad q_{\text{Coul}} = q^-, \quad (28)$$

respectively. The solution given by equations (21) remains unchanged, with  $T$  being the temperature of the proton component,

$$T_p = T_{p1} r^{-1}, \quad (29)$$

$$T_{p1} = 2T_1, \quad (30)$$

and the temperature of the electrons is

$$T_e = T_{e1} r^{-1/2}, \quad (31)$$

$$kT_{e1} = \left( \frac{Q_{\text{Coul}}}{Q_{\text{ff,R}}} \frac{m_e^2 c^2}{m_p} kT_1 \right)^{1/2}. \quad (32)$$

The obtained hot brake solution has the remarkable property that all the quantities are uniquely determined by a single parameter  $s$  — the dimensionless spin of the central object — specified on the inner boundary. The fact that the solution does not depend on the outer boundary condition in any way means that there is no simple way to match it to the external medium. Clearly, there has to be a second solution to bridge the gap between this solution and the external medium. We derive the bridging solution now.

## 4 Matching the hot brake flow with external medium

We assume that the spinning star is immersed in a uniform external medium with a density  $\rho_{\text{ext}}$ , temperature  $T_{\text{ext}}$  and pressure  $p_{\text{ext}}$ . We seek an accretion flow solution that extends from the spinning star on the inside to the external medium on the outside. As we have seen above, there is the self-similar hot brake solution extending from the boundary layer  $R \sim R_*$  outward through a large distance, at least a few hundred  $R_*$  or more. However, this self-similar solution has the surprising property that the density, temperature and angular velocity of the gas at any radius are completely independent of the outer boundary conditions. Hence, the solution cannot be matched to a



general external medium. We resolve this paradoxical situation by showing that there is a second self-similar solution which bridges the gap between the original solution and the external medium (see Narayan & Medvedev 2003). This new solution has an extra degree of freedom which permits it to match general outer boundary conditions.

We consider next the gas that lies just outside the region of validity of the first self-similar solution described above. In this zone, the pressure is expected to be approximately equal to the external pressure  $p_{\text{ext}}$ :

$$\rho c_s^2 = p_{\text{ext}} = \text{constant}. \quad (33)$$

This condition replaces the hydrostatic equilibrium equation (18), while equations (19) and (20) continue to be valid. In this region, we find that there is a second self-similar solution of the form

$$\rho = \rho_2 r^{-7/2}, \quad T = T_2 r^{7/2}, \quad \Omega = \Omega_2 r^{-9/4}, \quad (34)$$

where the label “2” refers to the fact that this is our second solution.

To match the second and first solutions, we require that the fluxes of angular momentum in the two solutions must be equal; this yields the constraint  $(3/2)\rho_1\Omega_1T_1^{1/2} = (9/4)\rho_2\Omega_2T_2^{1/2}$ . Making use of this and the other equations, we solve for the numerical coefficients in equation (34):

$$\rho_2 = \frac{\alpha^{3/2}s^3}{p_{\text{ext}}^{1/2}R_g^{3/2}} \frac{3^{5/2}}{2^{9/4}} \left(\frac{m_e}{m_p}\right)^{3/4} \frac{c^4}{Q_{\text{ff,NR}}^{3/2}}, \quad (35)$$

$$kT_2 = \frac{p_{\text{ext}}^{3/2}R_g^{3/2}}{\alpha^{3/2}s^3} \frac{2^{5/4}}{3^{5/2}} \left(\frac{m_p}{m_e}\right)^{3/4} \frac{m_p Q_{\text{ff,NR}}^{3/2}}{c^4}, \quad (36)$$

$$\Omega_2 = \frac{\alpha^{1/4}s^{3/2}}{p_{\text{ext}}^{1/4}R_g^{5/4}} 2^{-3/8} 3^{-3/4} \left(\frac{m_e}{m_p}\right)^{1/8} \frac{c^2}{Q_{\text{ff,NR}}^{1/4}}. \quad (37)$$

The pressure in this solution is constant and equal to the external pressure,  $p_{\text{ext}}$ , and the angular momentum flux is also constant and is equal to  $\dot{J}$  in equation (26). If the flow has a small but nonzero accretion rate,  $\dot{m} \neq 0$ , then its radial velocity varies as [see eq. (17)]

$$v \propto r^{3/2}. \quad (38)$$

Whereas the original hot brake self-similar solution has a unique profile for a given choice of  $s$ , we see that the second solution derived here has an extra

degree of freedom, namely the external pressure  $p_{\text{ext}}$ . This extra degree of freedom solves the problem discussed above. Thus, the full solution consists of two zones: an inner zone described by the first (Medvedev & Narayan 2001a) solution (21) and an outer zone described by the second solution (34). The radius  $r_{\text{match}}$  at which the two solutions match is obtained by equating the pressures:

$$r_{\text{match}} = \frac{\alpha^{1/3} s^{2/3}}{p_{\text{ext}}^{1/3} R_g^{1/3}} \frac{3^{1/3}}{2^{7/6}} \left( \frac{m_e}{m_p} \right)^{1/6} c^{5/3} Q_{\text{ff,NR}}^{1/3}. \quad (39)$$

The second solution matches the external medium at the radius  $r_{\text{ext}}$  at which its temperature matches that of the medium. This gives

$$r_{\text{ext}} = \frac{\alpha^{3/7} s^{6/7}}{p_{\text{ext}}^{3/7} (kT_{\text{ext}})^{2/7} R_g^{3/7}} \frac{3^{5/7}}{2^{5/14}} \left( \frac{m_e}{m_p} \right)^{3/14} \frac{c^{8/7}}{m_p Q_{\text{ff,NR}}^{3/7}}. \quad (40)$$

If we wish we could also write this in terms of the external density by making the substitution  $kT_{\text{ext}} = m_p p_{\text{ext}} / 2\rho_{\text{ext}}$ .

## 5 External medium solution

For completeness, we present here the solution inside the external medium (Narayan & Medvedev 2003). By assumption, the external medium has a uniform temperature and density, and a uniform rate of cooling. To maintain equilibrium, there has to be some constant source of heat that exactly compensates for the cooling. We assume that such a source of heat exists (e.g., cosmic rays). The rotation  $\Omega$  is non-zero, but it decays rapidly outward. The small amount of rotation helps to transport the angular momentum flux from the star out into the external medium. Solving the angular momentum conservation law (3), we obtain the following solution

$$\rho = \rho_{\text{ext}}, \quad T = T_{\text{ext}}, \quad \Omega = \Omega_3 r^{-4}, \quad (41)$$

where

$$\Omega_3 = \alpha s^3 \frac{3^{5/2}}{2^7 \pi} \frac{m_e^{1/2} c^5}{R_g^2 Q_{\text{ff,NR}}} \rho_{\text{ext}}^{-1} (kT_{\text{ext}})^{-1/2}, \quad (42)$$

and  $p_{\text{ext}} = 2kT_{\text{ext}}\rho_{\text{ext}}/m_p$ . For  $\dot{m} \neq 0$ , the velocity scales as  $r^{-2}$ .

We confirm the existence and the structure of our matching solution (and the external medium) using the same numerical model (Narayan & Medvedev 2003). In the calculations, the flow was taken to extend from an inner radius  $R_{\text{in}} = 3 R_g$  to  $R_{\text{out}} = 10^7 R_g$ . The mass accretion rate was taken to be low,  $\dot{m} = 2 \times 10^{-5}$ , in order that the flow should correspond to the regime of the hot settling flow solution. We took the viscosity parameter to be  $\alpha = 0.1$  and set the spin of the star to be  $s = 0.3$  (i.e., 30% of the Keplerian rotation at the stellar surface). We took the other inner boundary conditions to be the same as in MN01. At the outer boundary, we specified the temperature and density of the external medium. Figure 3 shows four solutions. The external temperature is kept fixed at  $T(R_{\text{ext}}) = 10^8$  K in all the solutions, but the external density varies by a decade and a half:  $\rho(R_{\text{ext}}) = 2.5 \times 10^9, 8.1 \times 10^8, 2.5 \times 10^8, 8.1 \times 10^7 \text{ cm}^{-3}$ . We have also done other calculations in which we kept  $\rho_{\text{ext}}$  fixed and varied  $T_{\text{ext}}$ . These give very similar results.

Fig. 3 shows that, right next to the star, there is a boundary layer, where the density rises sharply as one goes into the star and the temperature drops suddenly. We do not analyze this region. Once we are outside the boundary layer, the gas behaves very much according to the analytical solutions discussed in Section 3.2. Starting just outside the boundary layer and extending over a wide range of radius, the numerical solution exhibits a self-similar behavior with power-law dependences of the density, temperature and angular velocity. This region corresponds to the self-similar solution of MN01. There are, in fact, two zones, an inner two-temperature zone, and an outer one-temperature zone (Medvedev & Narayan 2001a) [see also Eq. (21)]. The most notable feature of this region is that the density, temperature and angular velocity of the numerical solutions are completely independent of the outer temperature and density, as predicted by the analytical solution. The slopes of the numerical curves also agree well with the analytical scalings.

At a radius  $R_{\text{match}} \sim 5 \times 10^4 \dots 2 \times 10^5 R_g$  [depending on the outer pressure, see Eq. (39)], solution 1 merges with solution 2 [Eq. (34)] described in the previous section. Here, the solution does depend on the outer boundary conditions, and it scales roughly according to the slopes derived analytically. At even larger radii  $R > R_{\text{ext}} \sim 3 \times 10^5 \dots 2 \times 10^6 R_g$  [see Eq. (40)], the flow matches onto the ambient external medium. In this region we have solution 3 [Eq. (41)] described in the present section. As expected, out here only the angular velocity and the radial velocity vary with radius. Both have the scalings predicted for solution 3.

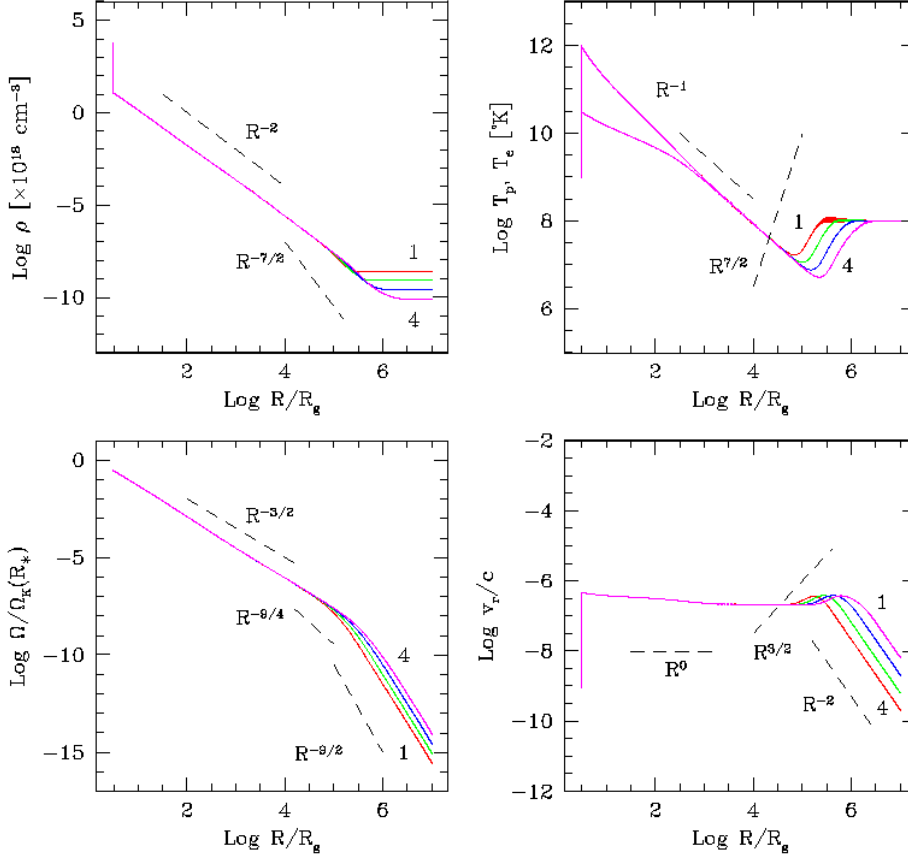


Figure 3: Profiles of density (top left panel), temperature (top right panel, the electron temperature is the lower curve on the left and the proton temperature is the higher curve), angular velocity (bottom left panel), and radial velocity (bottom right panel), for four numerical solutions of the full height-integrated differential equations. The four solutions correspond to different values of the density of the external medium:  $\rho_{\text{ext}} = 2.5 \times 10^9, 8.1 \times 10^8, 2.5 \times 10^8, 8.1 \times 10^7 \text{ cm}^{-3}$ . The first and fourth solutions are labeled 1 and 4, respectively. The temperature of the external medium and the accretion rate are kept fixed in all the solutions:  $T_{p,\text{ext}} = T_{e,\text{ext}} = 10^8 \text{ K}$ ,  $\dot{m} = 2 \times 10^{-5}$ . The analytical slopes of the three self-similar solutions are shown for comparison

## 6 Boundary layer solution

Finally we discuss the last piece: the structure of the boundary layer. Unlike the previous cases, the solution to the boundary layer (BL) cannot be obtained in a self-similar form in terms of the radial coordinate  $R$ . The structure of the BL is intrinsically non-self-similar in  $R$  since all the gas parameters (e.g., the temperature, gas density, etc.) change very dramatically over a relatively short radial region:  $R_* \leq R \lesssim 2R_*$ , as can be seen from the numerical solutions discussed in the previous sections. For instance, the density nearly diverges as one gets close to the star surface whereas the temperature decreases to the values well below the virial temperature. Such a behavior, however, suggests to look for a self-similar solution in terms of the distance from the stellar surface, i.e., in terms of  $D = R - R_*$ . In this calculation we neglect the effects of radiation transfer and, especially, the Comptonization. They may be important in hot regions, but will unlikely strongly affect the flow closer to the star, where the temperature of the gas falls below  $\text{few} \times 10^9$  K or so (see discussion in Section 7.2.3).

Unlike all previous cases, here we cannot neglect the radial (infall) velocity. For simplicity, we consider the one-temperature case. The generalization to the two-temperature case is straightforward: it follows from the equality of the Coulomb energy transfer rate and the heating/cooling rates (see Section 3.2) and will be discussed in a separate paper. We again use the height-integrated hydrodynamic equations, but now written in the approximation that  $R = R_* + D$  with  $D \ll R_*$ :

$$-\dot{M} = 4\pi R_* \rho v, \quad (43)$$

$$v \frac{dv}{dD} = (\Omega^2 - \Omega_{K*}^2) R_* - \frac{1}{\rho} \frac{d}{dD} (\rho c_s^2), \quad (44)$$

$$4\pi\alpha (\rho c_s^2) \frac{R_*^4}{\Omega_{K*}} \frac{d\Omega}{dD} = \dot{J} - \dot{M} \Omega R_*^2, \quad (45)$$

$$\frac{\rho v}{\gamma - 1} \frac{dc_s^2}{dD} - c_s^2 v \frac{d\rho}{dD} = q^+ - q^-, \quad (46)$$

where

$$q^+ = \alpha (\rho c_s^2) \frac{R_*^2}{\Omega_{K*}} \left( \frac{d\Omega}{dD} \right)^2, \quad (47)$$

$$q^- = Q_{\text{ff,NR}} \rho^2 \sqrt{c_s^2}, \quad (48)$$

and in equation (43) we took into account that the radial velocity is negative (inward).

As we mentioned above, we are looking in the solution which is self-similar in  $D$ , that is the temperature, density, angular and radial velocities are expressed as power-laws. In addition, we must satisfy the boundary condition at the star surface:  $\Omega = \Omega_*$ . Thus, we readily conclude that  $\Omega \propto D^0$  (otherwise it is either zero or diverges at  $D = 0$ , i.e.,  $R = R_*$ ).

Let us now consider equation (44). First, we note that the rotation is sub-Keplerian,  $\Omega_*^2 \ll \Omega_{K*}^2$  so that we neglect this term. Next, we cast it into the form:

$$\frac{d}{dD} \left( c_s^2 + \frac{1}{2} v^2 \right) + c_s^2 \left( \frac{1}{\rho} \frac{d\rho}{dD} + \frac{1}{2} \frac{v_{\text{ff},*}}{c_s^2} \right) = 0, \quad (49)$$

where  $v_{\text{ff},*} = \sqrt{2}\Omega_{k*}R_*$  is the free-fall velocity that near the stellar surface. We now make the following assumptions, which consistency with the obtained solution must be checked *a posteriori*: (i) the flow is always subsonic,  $v^2 \ll c_s^2$ , and (ii)  $c_s^2$  grows with  $D$  slower than linearly (for  $c_s^2 \propto D^{2\beta}$  we should have  $2\beta < 1$ ), then the second term in the second brackets is sub-dominant and may be neglected as well. With these assumptions, the equation simplifies to

$$\rho c_s^2 = p = \text{const.}, \quad (50)$$

that is, the pressure is constant throughout the boundary layer.

Considering equation (45), we notice that since  $\Omega = \text{const.}$ , its radial derivative vanishes,  $d\Omega/dD = 0$ , and the equation simply defines the angular momentum flux,  $\dot{J} = \dot{M}\Omega_*R_*^2$ . By the same token, the heating rate in equation (46) vanishes. Together with the continuity equation (43), the energy equation reads,

$$\frac{\dot{M}}{4\pi R_*^2} \left( \frac{1}{\gamma - 1} \frac{d c_s^2}{dD} - \frac{c_s^2}{\rho} \frac{d\rho}{dD} \right) = Q_{\text{ff,NR}} \rho^2 c_s \quad (51)$$

The system of equations (43), (50), (51), together with  $\Omega = \Omega_*$  admits the following self-similar solution:

$$\rho = \rho_0 d^{-2/5}, \quad T = T_0 d^{2/5}, \quad v = v_0 d^{2/5}, \quad \Omega = \Omega_0 d^0, \quad (52)$$

where we used the dimensionless distance  $d = D/R_*$ . The constant factors are (recall that  $c_s^2 = kT/m_p$ ):

$$\rho_0 = \frac{p_{\text{out}}}{B^2}, \quad kT_0 = m_p B^2, \quad v_0 = \frac{\dot{M}}{4\pi R_*^2 \rho_0}, \quad \Omega_0 = \Omega_*, \quad (53)$$

where we denoted

$$B = 10\pi Q_{\text{ff,NR}} \left( \frac{\gamma}{\gamma - 1} \right) \frac{R_*^3}{\dot{M}} \quad (54)$$

and  $p_{\text{out}}$  is the pressure on the outside of the boundary layer, where it should match to the pressure on the inside of the hot brake flow. Using equations of section 3.2, we can calculate this pressure to be equal to

$$p_{\text{out}} = \frac{3}{16\sqrt{2}} (\alpha s^2) \frac{Q_{\text{ff,NR}} c^5}{R_g} \left( \frac{R_g}{R_*} \right)^3 \left( \frac{m_e}{m_p} \right)^{1/2}. \quad (55)$$

With the solution we check that the assumptions made in order to simplify equation (49) are consistent: indeed  $v^2/c_s^2 \propto d^{2/5} \rightarrow 0$  as  $d \rightarrow 0$  and  $2\beta = 2/5 < 1$ . There is a little subtlety with Eq. (49), namely the condition  $\rho c_s^2 = \text{const.}$  ensures that the two leading terms cancel each other exactly and it looks like we need to keep higher order terms, e.g., those that have been dropped out. Apparently, it is important to understand that the presented self-similar solution is approximate: the flow is pressure-dominated but with  $\rho c_s^2 \approx \text{constant}$ . A small deviation from the exact equality is necessary to compensate for the remaining next order terms.

Using our computer code, we calculated the structure of the boundary layer numerically and presented it in Figure 4. Note the remarkable agreement of this numerical solution with the theoretical one:  $\Omega = \text{const.}$ ,  $p \approx \text{const.}$ , and  $\rho$ ,  $T_p$ ,  $v$  follow the predicted scalings.

## 7 Properties of the hot brake accretion flow

### 7.1 Stability of the flow

The existence of a mathematical solution to hydrodynamic equations does not imply that the corresponding accretion flow may realize in nature. If the flow is unstable to a certain type of instability, this instability may dramatically change the structure of the entire flow, or even prohibit it from being realized in nature. Here we perform the linear stability analysis of the hot brake flow.

#### 7.1.1 Stability to winds/outflows

It is known that the Bernoulli parameter of the accreting gas in BH ADAFs is positive for a wide range of  $r$  (Narayan & Yi 1994, 1995a; Narayan, Kato & Honma

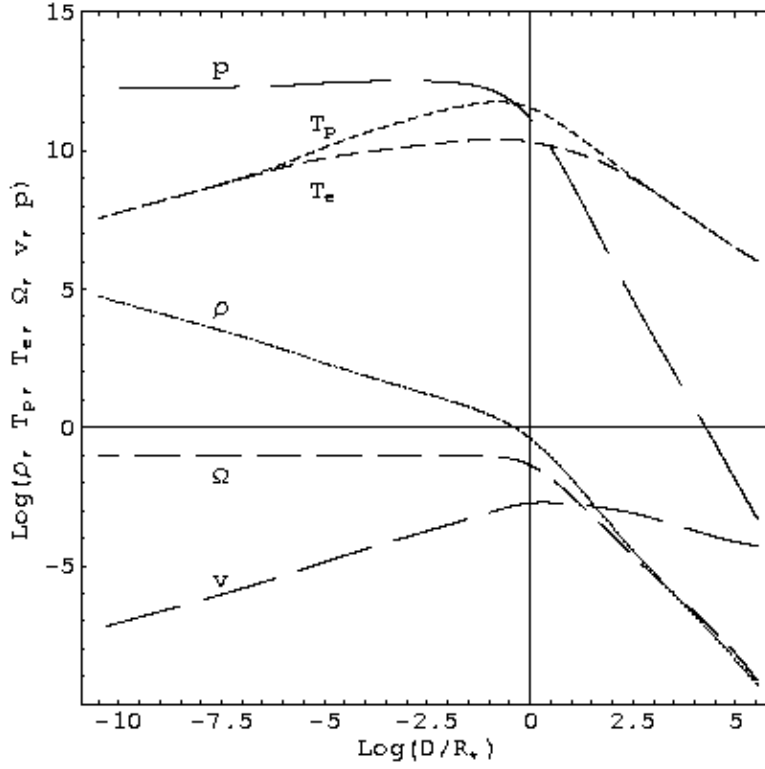


Figure 4: The structure of the boundary layer.  $\text{Log}$  of  $\rho$ ,  $T_e$ ,  $T_p$ ,  $\Omega$ ,  $v$  and  $p = \rho c_s^2$  as functions of  $\text{Log}(D/R_*)$  are shown for  $\dot{m} = 0.01$ ,  $\alpha = 0.1$ ,  $s = 0.1$ .



1997), and it has been suggested that the positive Bernoulli parameter may trigger strong winds or jets in these systems (Narayan & Yi 1994, 1995a; Blandford & Begelman 1999, but see Abramowicz, et al. 2000). Igumenshchev & Abramowicz (1999, 2000) confirmed with numerical simulations that strong outflows are produced from BH ADAFs when  $\alpha \sim 1$ .

Normalizing the Bernoulli parameter,  $Be$ , by  $(\Omega_K R)^2$ , and using equations (21),(24), we find that the self-similar hot brake flow has

$$\begin{aligned} b \equiv \frac{Be}{\Omega_K^2 R^2} &= \frac{1}{v_K^2} \left( \frac{1}{2} v^2 + \frac{1}{2} \Omega^2 R^2 - \Omega_K^2 R^2 + \frac{\gamma}{\gamma - 1} c_s^2 \right) \\ &\simeq -\frac{2\gamma - 3}{3(\gamma - 1)}, \end{aligned} \quad (56)$$

where  $\gamma$  is the mean adiabatic index of the flow.

The right hand side of equation (56) can be either positive or negative, depending on the value of  $\gamma$ . Hence, we find that the gas is gravitationally bound and unable to flow out in a wind (i.e.  $b < 0$ ) if the adiabatic index satisfies

$$\gamma > \frac{3}{2}; \quad (57)$$

that is, the accretion flow can produce a wind and/or a collimated outflow only if  $\gamma$  is well below that of an ideal gas ( $\gamma = 5/3$ ) and is stable to such outflows if  $\gamma > 1.5$ . Normally, we expect  $\gamma$  to be close to  $5/3$  for the accreting gas.

### 7.1.2 Stability to convection

It is well known that if the entropy increases inward in a gravitationally-bound non-rotating system, the gas is convectively unstable; otherwise the flow is stable. The specific entropy profile in the settling accretion flow around a NS can be readily calculated from equations (4),(5) using (21),(24). This gives

$$\frac{ds}{dR} = \frac{k}{m_p} \frac{1}{\gamma - 1} \frac{d}{dR} \ln \left( \frac{c_s^2}{\rho^{\gamma-1}} \right) = \frac{k}{m_p} \frac{2\gamma - 3}{\gamma - 1} \frac{1}{R}. \quad (58)$$

We see that the entropy increases outward for  $\gamma > 1.5$  and inward for  $\gamma < 1.5$ . Hence if  $\gamma > 1.5$  the flow is stable against convection, while if  $\gamma < 1.5$  the flow is convectively unstable.

In the presence of rotation, the analysis is a little more complicated. Narayan et al. (2000) and Quataert & Gruzinov (2000) discuss the generalization of the Schwarzschild criterion for accretion flows with rotation. If the gas motions are restricted to the equatorial plane of a height-integrated flow, convective stability requires the following effective frequency to be positive:

$$N_{\text{eff}}^2 = N^2 + \kappa^2 > 0, \quad (59)$$

where  $N$  is the Brunt-Väisälä frequency and  $\kappa$  is the epicyclic frequency,  $\kappa = \Omega$  for  $\Omega \propto R^{-3/2}$ . For a power-law flow with  $\rho \propto R^{-a}$  and  $\Omega(R) = s\Omega_K \propto R^{-3/2}$  with  $s^2 = 1 - (1+a)c_0^2$ , this criterion may be written as follows (see Narayan et al. 2000 for more discussion)

$$N_{\text{eff}}^2 = \Omega_K^2 \left( -[(\gamma + 1) - a(\gamma - 1)] \frac{(1+a)c_0^2}{\gamma} + 1 \right) > 0. \quad (60)$$

Since for the self-similar settling solution  $a = 2$ , the stability criterion (60) becomes

$$N_{\text{eff}}^2 \approx \frac{\Omega_K^2}{\gamma} (2\gamma - 3) > 0 \quad (61)$$

which yields that the flow is convectively stable if

$$\gamma > \frac{3}{2}. \quad (62)$$

This condition is different from the stability criterion against outflows, given in equation (57).

Following the techniques developed by Quataert & Gruzinov (2000), Narayan et al. (2000) have also presented a more general analysis of convection in a self-similar accretion flow. This analysis, which does not restrict motions to lie in the equatorial plane, assumes that  $v_\phi$  and  $c_s$  are independent of the polar angle  $\theta$  (as is valid for a marginally convectively stable system, cf Quataert & Gruzinov 2000). Narayan et al. (2000) find that the most unstable region of the flow is near the rotation axis,  $\theta = 0, \pi$ . They show that the marginal stability criterion for this polar fluid coincides with the condition for the positivity of the Bernoulli parameter. That is, a flow which is convectively stable at all  $\theta$  has a negative Bernoulli parameter, while a flow which is convectively unstable for at least some values of  $\theta$  has a positive Bernoulli parameter. (The Bernoulli parameter itself is independent of  $\theta$ .)

We have verified this result for the solutions presented in this paper. Specifically, when we apply to our solution the more general convective stability criterion given by equation (A9) of Narayan et al. (2000), we recover the condition (57) above.

### 7.1.3 Thermal stability

Not all hot accretion flows are stable. For instance, the cooling-dominated SLE solution has been shown to be thermally unstable (Piran 1978; Wandel & Liang 1991; Narayan & Yi 1995b) and, hence, unlikely to exist in nature. More generally, it has been shown that any accretion flow in which heating balances cooling is thermally unstable if the cooling is due to bremsstrahlung emission (Shakura & Sunyaev 1976; Piran 1978). The ADAF solution, on the other hand, is known to be thermally stable (Narayan & Yi 1995b; Kato et al. 1996, 1997). In this solution, cooling is weak (ideally zero), and so the thermal energy of the flow is not radiated but is advected with the gas (hence the name). The CDAF is also believed to be stable, since in this flow again the thermal energy is advected by convective eddies and is either carried into the black hole or is radiated near the outer boundary of the flow (Ball, Narayan & Quataert 2001). In contrast to these radiatively inefficient flow, the hot brake flow is cooling-dominated. Energetically, this flow is very similar to the SLE solution, since the heat energy produced by viscous dissipation is radiated locally via bremsstrahlung. Therefore, in analogy with the SLE solution, one might expect the flow to be thermally unstable. However, this is not necessarily the case, as we show in this section (see also, Medvedev & Narayan 2001b).

The physics of the thermal instability is simple (Field 1965). Suppose a system is in thermal equilibrium, so that the rates of heating and cooling per unit volume are equal:  $Q^+ = Q^-$ . For simplicity let us take the heating and cooling rates to be functions of only the local temperature:  $Q^+ \propto T^\alpha$ ,  $Q^- \propto T^\beta$  ( $\alpha, \beta > 0$  for concreteness).

Suppose, with increasing temperature, the cooling rate rises faster than the heating rate, i.e.,  $\beta > \alpha$ . Then a local perturbation which causes a small increase in the temperature will result in a net cooling of the gas:  $Q^- > Q^+$ . This will cause the temperature to return to its equilibrium value, which means that the gas will be thermally stable. (It is easily seen that this is true also for a small decrease in the temperature.) On the other hand, if  $\alpha > \beta$ , the gas is thermally unstable. For instance, if the temperature

decreases slightly, cooling becomes stronger than heating and the system deviates from its equilibrium in a run-away manner.

When a gas is hot, one should always include the effect of thermal conduction, — being usually a strong function of temperature, thermal conduction may (and will) affect the accretion flow structure and, especially, its stability.

It is easy to see that thermal conduction will tend to reduce the thermal instability. An unstable thermal mode of wave-vector  $k$  consists of a growing temperature perturbation of wave-length  $2\pi/k$ . Thermal conduction tends to smooth out this temperature perturbation through heat diffusion. If the rate at which the temperature perturbation grows is smaller than the rate at which it is smoothed out by conduction, then the instability will be suppressed and the mode will be stable. Otherwise, the mode will continue to grow, but at a somewhat reduced rate.

The rate at which fluctuations are smoothed out by conduction depends on the spatial scale of the perturbation. The smaller the scale (i.e. the larger the value of  $k$ ), the faster the conduction, and the greater the stabilizing effect. Thus, we expect conduction to stabilize thermal modes with  $k$  greater than some critical  $k_{\text{crit}}$ . Our task in this section is to estimate  $k_{\text{crit}}$  through a quantitative analysis. If we find that  $k_{\text{crit}}R \gg 1$ , then we conclude that the flow is thermally unstable. On the other hand, if we find that  $k_{\text{crit}}R \lesssim 1$ , we may reasonably claim that the flow is thermally stable. Technically, for  $k \sim 1/R$ , we need to carry out a global analysis rather than the local analysis presented in this paper, but this is beyond the scope of the present section.

Let us write the heat flux  $q$  due to thermal conduction as

$$q_{\text{cond}} = -\kappa \nabla T, \quad (63)$$

where  $\kappa$  is the thermal conductivity coefficient. Thermal conductivity in a dense, fully ionized gas is given by the Spitzer (1962) formula,

$$\kappa_{\text{Sp}} \approx 1.3nk_B v_T \lambda \simeq 6.2 \times 10^{-7} T_e^{5/2} \text{ erg}/(\text{s K cm}). \quad (64)$$

Here  $v_T = (k_B T_e / m_e)^{1/2}$  is the electron thermal speed,  $T_e$  is the electron temperature ( $T_e = T$  for a one-temperature plasma),  $k_B$  is the Boltzmann constant, and

$$\lambda \simeq 10^4 T_e^2 / n \text{ cm} \quad (65)$$

is the electron mean free path. Note that  $\lambda$  is independent of the mass of the particle.

In the collisionless regime, i.e., when the mean free path of an electron becomes comparable to or larger than the temperature gradient scale  $\lambda \gtrsim T_e/|\nabla T_e|$ , equation (63) for the heat flux is no longer valid. For an unmagnetized plasma, the heat flux takes the following saturated form (Cowie & McKee 1977),

$$q_{\text{sat}} \simeq -C\rho c_s^3 \text{sgn}(\nabla T), \quad (66)$$

where  $C \sim 5$  is a numerical constant whose exact value depends on the particle distribution function. This result is not relevant for our problem since our plasma is magnetized.

For a collisionless magnetized plasma, thermal conduction is anisotropic. Electrons stream freely along the field lines, and the parallel heat flux remains the same as for the unmagnetized case described above. However, the transverse heat flux is greatly reduced because electrons are tied to the field lines on the scale of the Larmor orbit. In fact, if the field is uniform and homogeneous, the perpendicular thermal flux is identically equal to zero since electrons cannot move across the field lines. In a tangled field, however, electrons can jump from one field line to another and thus conduct heat perpendicular to the field. Since we are dealing with a turbulent accretion flow with a tangled magnetic field, this is the regime of interest to us.

The physics of this regime of conduction has been discussed by Rechester & Rosenbluth (1978); Chandran & Cowley (1998); Medvedev & Narayan (2001b), who identified two important effects, which we discuss now.

First, since particles can move freely only along field lines, the characteristic effective mean free path is set by the correlation scale of the magnetic field  $l_B$ . In a hot accretion flow this scale is not known in general. However, it is likely that turbulent motions in the flow occur on a scale comparable to the local radius  $R$ , since this is the only characteristic scale in the problem. Very likely, the turbulent magnetic field will also have the same scale  $l_B \sim R$ . We parameterize this scale as  $l_B = \xi R$ . We expect  $\xi \leq 1$  because turbulent fluctuations cannot have a scale larger than the local radius of the flow. We assume  $\xi \sim 0.1$  throughout the paper.

Second, the magnetic field is inhomogeneous. Therefore, only a fraction  $\vartheta < 1$  of the particles will be able to pass through the magnetic mirrors that will be present in the field, and it is only these particles that transport energy beyond a distance  $\sim l_B$ . For magnetic field strength fluctuations  $\delta B \sim \langle B \rangle$ , the fraction of free streaming particles is estimated to be  $\vartheta \sim 0.3$ .

Typically, hot accretion flows are highly collisionless, i.e.,  $\lambda \gg R \gtrsim l_B$ . Therefore, we can write the thermal conduction coefficient as

$$\kappa_B \simeq nk_B v_T l_B \vartheta \simeq 10^{-2} nk_B v_T R \xi_{-1} \vartheta_{-1}, \quad (67)$$

where  $\xi_{-1} = \xi/10^{-1}$  and  $\vartheta_{-1} = \vartheta/10^{-1}$ . Let us write the conductive heat flux in a form similar to that used for the viscous stress, namely

$$q_{\text{cond}} = -\alpha_c \frac{c_s^2}{\Omega_K} \rho \frac{dc_s^2}{dx}, \quad (68)$$

where the dimensionless coefficient  $\alpha_c$  is analogous to the Shakura-Sunyaev viscosity parameter  $\alpha$ , and is given by

$$\alpha_c \simeq \frac{R}{H} \xi \vartheta \simeq 10^{-2} \xi_{-1} \vartheta_{-1}. \quad (69)$$

Here we have used the fact that  $v_T \simeq c_{se}$  and  $H/R \sim c_s/v_{\text{ff}} \sim c_s/\Omega_K R$ , where  $H$  is the accretion disk scale height (in hot flows,  $H \sim R$ ) and  $v_{\text{ff}}$  is the free-fall speed.

To study the thermal stability of an accretion flow, we need to include additional physics, namely the effects of shear and rotation. We use the shearing sheet approximation (Goldreich & Lynden-Bell 1965; Julian & Toomre 1966; Goldreich & Tremaine 1978), which is a convenient way of introducing the relevant physics without unnecessary technical complications. Furthermore, we carry out a local WKB analysis under the assumption that the wavelength of the perturbation is much smaller than the radius.

The shearing sheet model approximates the flow as locally flat, neglecting the effects of the flow curvature. Conventionally, the shearing sheet coordinates are Cartesian with  $x$ ,  $y$ ,  $z$  corresponding to the radial, azimuthal, and vertical directions, respectively, centered on some point in the flow at a radius  $R$ . These coordinates are appropriate for describing the motion of a parcel of gas whose geometrical size is small compared to the local radius,  $R$ , of the flow (i.e.,  $x$ ,  $y$ ,  $z \ll R$ ), so that the effects of geometry and curvature are insignificant. We neglect viscosity in the azimuthal momentum equation; of course, we do include viscous dissipation in the energy equation, where it plays an important role.

It is convenient to compare the wave-vector  $k$  of a perturbation with  $1/R$  and the frequency of a mode with the local Keplerian frequency  $\Omega_K = \sqrt{GM_*/R^3}$ , where  $M$  is the mass of the central object. The shearing sheet

approximation is accurate for “local” small-scale perturbations with  $kR \gg 1$ . Perturbations with  $kR \sim 1$  are global; their properties may be understood only through a global stability analysis, usually numerical, which we do not attempt here.

We consider a shearing gas flow with unperturbed velocity given by

$$\mathbf{V}_0(x) = 2A x \hat{y}, \quad (70)$$

where  $2A = d\mathbf{V}_0/dx$  is the shear frequency and “hat” denotes a unit vector. Note that we have neglected the radial velocity in the equilibrium flow since this component of the velocity is significantly smaller than the azimuthal velocity. To include the effect of rotation we assume that there is a Coriolis acceleration, described by an angular rotation frequency  $\boldsymbol{\Omega} = \Omega \hat{z}$ . The vorticity and epicyclic frequency are then given by

$$2B = 2A + 2\Omega, \quad \kappa_{\text{epi}} = 2(\Omega B)^{1/2}. \quad (71)$$

The hot brake flow satisfies the Keplerian scaling,  $\Omega \propto R^{-3/2}$ . Therefore, we have  $2A = -(3/2)\Omega$ ,  $2B = \Omega/2$  and  $\kappa_{\text{epi}} = \Omega$ .

We assume that perturbations in the flow have structure only in the  $x$  direction, and we ignore motions in the  $z$  direction. We write the perturbations (represented by primes) in the velocity, density and sound speed as

$$\mathbf{V}'(x, t) = u(x, t) \hat{x} + v(x, t) \hat{y}, \quad (72)$$

$$\rho'(x, t) = \rho_0 \sigma(x, t), \quad (73)$$

$$c_s'^2(x, t) = a^2(x, t), \quad (74)$$

where  $\rho_0$  and  $c_s^2$  are the equilibrium values of the density and the square of the sound speed. Note that we define  $c_s$  to be the isothermal sound speed, so that the pressure is written as  $p = \rho c_s^2$ . By considering perturbations of the basic hydrodynamic equations, namely the continuity, radial momentum, azimuthal momentum and entropy equations, we obtain the following four linearized equations (note that in the presence of conduction the energy equation has an additional contribution from the divergence of  $q_{\text{cond}}$ , and in equilibrium, the total heating is equal to the total cooling),

$$\frac{\partial \sigma}{\partial t} + \frac{\partial u}{\partial x} = 0, \quad (75)$$

$$\frac{\partial u}{\partial t} - 2\Omega v + c_s^2 \frac{\partial \sigma}{\partial x} + \frac{\partial a^2}{\partial x} = 0, \quad (76)$$

$$\frac{\partial v}{\partial t} + 2Bu = 0, \quad (77)$$

$$\frac{\rho_0}{\gamma - 1} \frac{\partial a^2}{\partial t} - \rho_0 c_s^2 \frac{\partial \sigma}{\partial t} = (Q^+ + Q^-)' + \alpha_c \frac{\rho c_s^2}{\Omega_K} \frac{\partial^2 a^2}{\partial x^2}, \quad (78)$$

where we have used  $d/dt = \partial/\partial t + V_{0x}\partial/\partial x \simeq \partial/\partial t$  since the inflow velocity  $V_{0x}$  is set to zero in our approximation.

For the heating and cooling rates, we make use of “realistic” expressions that represent the physics of viscous accretion flows. Thus we write

$$Q^+ = \alpha \frac{\rho c_s^2}{\Omega_K} \left( \frac{dV_{0y}}{dx} \right)^2 = 4\alpha A^2 \frac{\rho c_s^2}{\Omega_K}, \quad Q^- = -\mathcal{C} \rho^2 (c_s^2)^n, \quad (79)$$

where  $\alpha \sim 0.1$  is the standard Shakura-Sunyaev viscosity parameter,  $V_{0y}$  is the  $y$ -component of the unperturbed velocity, and  $\mathcal{C}$  is a constant. We leave the index  $n$  in the cooling function unspecified for now, but we note that  $n = 1/2$  corresponds to non-relativistic free-free (bremsstrahlung) cooling.

We assume that the perturbations in equations (75) are of the form  $\exp(-i\omega t + ikx)$ . Substituting in the above equations and solving, we obtain the following dispersion relation (Medvedev & Narayan 2001b):

$$\omega \left[ \frac{\omega}{\gamma - 1} + \frac{i(n-1)}{\tau_{\text{cool}}} + \frac{ik^2 R^2}{\tau_{\text{cond}}} \right] (\omega^2 - \kappa_{\text{epi}}^2 - k^2 c_s^2) - \omega \left[ \omega + \frac{i(2B/A - 1)}{\tau_{\text{cool}}} \right] k^2 c_s^2 = 0, \quad (80)$$

where

$$\tau_{\text{cool}} = \left( \frac{\rho_0 c_s^2}{Q_0^\mp} \right) = \frac{\Omega_K}{4A^2 \alpha} = \frac{4}{9\alpha s^2} \Omega_K^{-1} \quad (81)$$

is the cooling (heating) time of the gas and

$$\tau_{\text{cond}} = \Omega_K R^2 / \alpha_c c_s^2 \quad (82)$$

is the conductive time scale.

The dispersion relation (80) corresponds to purely radial perturbations. The same relation can be used also for perturbations in the vertical direction, except that we must set  $\kappa_{\text{epi}} = 0$ . Perturbations in the azimuthal direction are more complicated. Because of the shear, a non-axisymmetric



wave packet is distorted as a function of time, and must be analyzed by special techniques which are beyond the scope of this study (see, e.g., Toomre 1977; Goldreich & Tremaine 1978).

Equation (80) is a fourth-order polynomial and has four roots corresponding to four modes. A flow is unstable if any of the four modes grows with time, i.e. if the corresponding root has  $\text{Im } \omega > 0$ . One of the roots of the dispersion relation is always  $\omega = 0$ . This root corresponds to the viscous mode, which in the present case is particularly simple because we neglected viscosity in the momentum equation. It is easy to show that if we introduce viscosity into the momentum equation the viscous mode would become stable, i.e., we will obtain  $\text{Im } \omega < 0$ . We do not consider the viscous mode further.

Let us now neglect thermal conduction for a moment,  $\tau_{\text{cond}} \rightarrow \infty$ . Then the physics of the remaining three modes may be understood by considering equation (80) in various limits. Consider first the limit  $k \rightarrow 0$ . In this limit, two of the roots are given by  $\omega = \pm \kappa_{\text{epi}}$ , corresponding to simple epicyclic oscillations. In the opposite limit  $k \rightarrow \infty$ , the same roots are given by  $\omega = \pm \gamma^{1/2} c_s k$ , which shows that they correspond to sound waves. In the absence of heating and cooling (i.e.  $\tau_{\text{cool}} \rightarrow \infty$ ), we can obtain an exact solution for these roots which is valid for all  $k$ :

$$\omega^2 = \kappa_{\text{epi}}^2 + \gamma c_s^2 k^2. \quad (83)$$

This is the standard dispersion relation for sound waves in a differentially rotating flow. The presence of  $\gamma$  is because the relevant sound speed is the adiabatic sound speed,  $\gamma^{1/2} c_s$  (recall that  $c_s$  is defined to be the isothermal sound speed).

The final root of the dispersion relation (80) corresponds to the thermal mode. In the limit  $k \rightarrow 0$ , we obtain

$$\omega = i(\gamma - 1) \frac{(1 - n)}{\tau_{\text{cool}}}. \quad (84)$$

We see that the mode is stable (for  $\gamma > 1$ ) if  $n > 1$  and unstable if  $n < 1$ . In the opposite limit  $k \rightarrow \infty$ , we find

$$\omega = i \frac{(\gamma - 1)}{\gamma} \frac{(2 - n - 2B/A)}{\tau_{\text{cool}}}. \quad (85)$$

Therefore, the mode is stable if  $n > 2(1 - B/A)$ , i.e.  $n > 8/3$  for our problem, and unstable otherwise. Note that an accretion flow that is cooled by free-free emission ( $n = 1/2$ ) is unstable in both limits.

Let us now turn the conduction back on. Figure 5 shows that the imaginary parts of all three modes decrease rapidly with increasing  $k$ . For the particular parameters we have selected, the growth rate of the unstable thermal mode (curve 3) goes to zero at  $k_{\text{crit}}R \sim 1.5$ , and the mode is stable for all  $k > k_{\text{crit}}$ .

We may also analyze equation (80) analytically. In the large- $k$  limit, the root corresponding to the thermal mode is equal to<sup>1</sup>

$$\omega = i \frac{(\gamma - 1)}{\gamma} \left( \frac{(2 - n - 2B/A)}{\tau_{\text{cool}}} - \frac{k^2 R^2}{\tau_{\text{cond}}} \right). \quad (86)$$

Clearly, for large  $k$ , conduction stabilizes the thermal mode, for the reasons explained at the beginning of this section. Using the above relation, we can estimate the critical  $k_{\text{crit}}$  above which all  $k$  are stable:

$$k_{\text{crit}}^2 R^2 = \frac{\tau_{\text{cond}}}{\tau_{\text{cool}}} \left( 2 - n - 2 \frac{B}{A} \right) = \frac{13}{6} \frac{\tau_{\text{cond}}}{\tau_{\text{cool}}}, \quad (87)$$

where we have substituted  $n = 1/2$  (free-free cooling) and  $B/A = -1/3$  (Keplerian scaling).

We should comment here that in the theory described above, the conductivity  $\kappa_B$  is a quantity averaged over many field correlation lengths. Therefore, the results of the stability analysis are valid only for perturbations on scales much larger than  $l_B$ . (This is somewhat inconsistent since we have assumed that  $l_B = \xi R \sim 0.1R$ .) For small-scale perturbations with  $k \gg (\xi R)^{-1}$ , the local magnetic field is nearly homogeneous. Therefore, thermal conductivity is anisotropic; its perpendicular component is of order of  $\kappa_B \sim n k_B v_T l_B \vartheta$  (for more discussion, see, Medvedev & Narayan 2001b), while the conductivity along the field lines is much larger:

$$\frac{q_{\parallel}}{q_{\perp}} = \frac{C \rho c_s^3 \text{sgn}(\nabla T)}{-\alpha_c (\rho c_s^2 / \Omega_K) (dc_s^2 / dx)} \sim \frac{C \rho c_s^3}{\alpha_c \rho c_s^3 (H/R)} \sim \frac{5}{\alpha_c} \gg 1,$$

---

<sup>1</sup>In deriving this equation from (80) we have used the fact that the acoustic time-scale is, in general, shorter than the time-scale of the thermal mode, i.e.,  $\omega \ll k c_s$ , and we have neglected  $\kappa_{\text{epi}}$  as before. In this case we can neglect  $\omega^2$  in the second brackets, so that equation (86) readily follows. It may seem that this procedure fails when the acoustic and thermal time-scales are comparable. This may happen when  $kR \sim 1$  (for such perturbations, the sound crossing time is of order the dynamical time) and when  $\tau_{\text{cool}}$  and  $\tau_{\text{cond}}$  are also comparable to the dynamical time, which is  $\sim \Omega_K^{-1}$ . Nevertheless, even in this case, equation (86) works fairly well near the stability threshold. Indeed, at the threshold itself,  $\text{Im } \omega = 0$ . Since further the thermal mode frequency has no real part, we have  $\omega \sim 0$  near the threshold; so we may safely neglect  $\omega^2$  compared to  $k^2 c_s^2$  in the second brackets of equation (86).

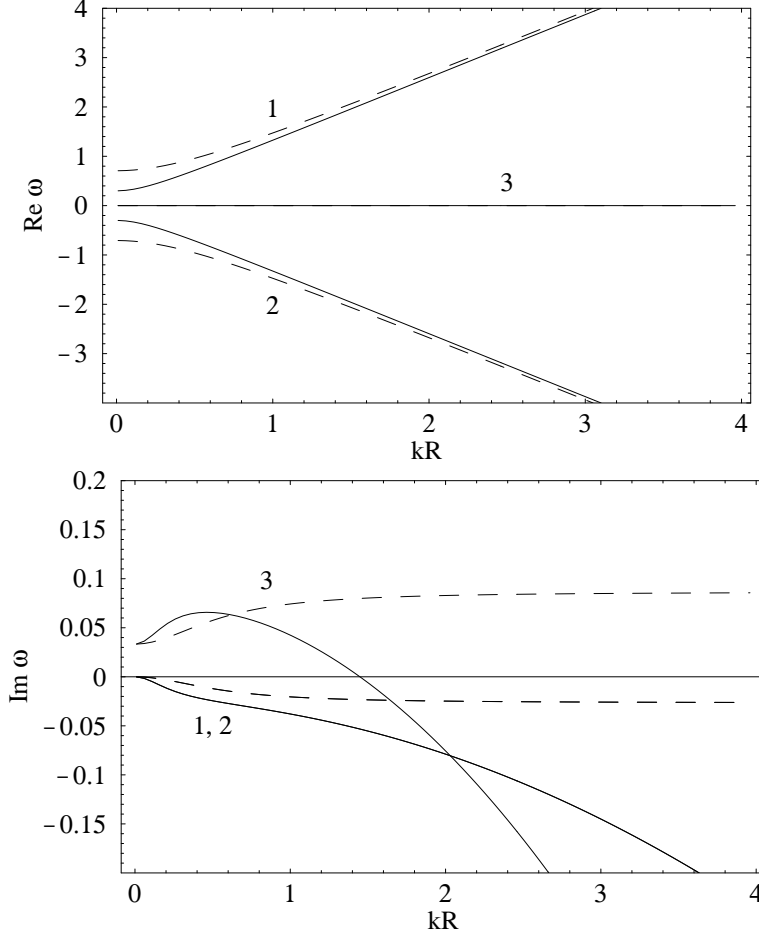


Figure 5: Real part (left panel) and imaginary part (right panel) of the frequencies of three modes. The curves labeled 1 and 2 refer to the two acoustic modes, and the curves labeled 3 refer to the thermal mode. The dashed curves correspond to the dispersion relation (80), which does not include thermal conduction  $\tau_{\text{cond}} \rightarrow \infty$ . The following parameter values were used:  $\kappa_{\text{epi}}/\Omega_K = s = \sqrt{0.5}$ ,  $\tau_{\text{cool,ff}} = 10\Omega_K^{-1}$ ,  $c_s = \Omega_K R$ ,  $\gamma = 5/3$ . The mode frequencies are normalized by the Keplerian frequency. The solid curves correspond to the dispersion relation (80), which includes thermal conduction. Here,  $\tau_{\text{cond}} = \tau_{\text{cool,ff}}$ , and the other parameters are the same as before.

as follows from equations (68) and (66). Thermal instability along the magnetic field lines is then suppressed more strongly than in the analysis presented above.

Thermal conduction in the hot brake flow is enormous (Medvedev & Narayan 2001b) due to the very high temperature and large mean free path of particles. The estimated value of thermal conduction is

$$\alpha_c \simeq \text{few} \times 10^{-2} \xi_{-1} \vartheta_{-1} \quad (88)$$

Is this level of thermal conduction enough to stabilize the thermal mode?

The relevant stability criterion is given in equation (87). However, before we apply this criterion, we need to allow for the fact that thermal conduction in the flow is so strong that it modifies even the equilibrium structure of the flow. In particular, the cooling time (81) is modified and becomes (Medvedev & Narayan 2001b)

$$\tau_{\text{cool}} = \frac{4}{(9\alpha s^2 + 2\alpha_c)} \Omega_K^{-1} \simeq \frac{2}{\alpha_c} \Omega_K^{-1}, \quad (89)$$

where we have assumed that  $\alpha_c \gg \alpha s^2$ , which is reasonable for typical parameters, e.g.  $\alpha \sim 0.1$ ,  $s \sim 0.1$ ,  $\alpha_c \sim 0.1$ . From equation (82) and using the self-similar solution from Section 3.2, we obtain the thermal conductive time<sup>2</sup>

$$\tau_{\text{cond}} = \frac{3}{\alpha_c} \Omega_K^{-1}, \quad (90)$$

Substituting  $\tau_{\text{cool}}$  and  $\tau_{\text{cond}}$  into the stability criterion (87), we then find

$$k_{\text{crit}} R = \left[ \frac{26\alpha_c}{9(9\alpha s^2 + 2\alpha_c)} \right]^{1/2} \simeq \sqrt{\frac{13}{9}} \simeq 1.2, \quad (91)$$

that is, thermal modes with  $kR \gtrsim 1$  are stable. This suggests that the hot brake flow with thermal conduction is stable to the thermal instability.

Whether the mode  $kR = 1$  itself is stable or not cannot be reliably determined from our local analysis. A global stability analysis is necessary to properly account for the effects of geometry and curvature, but this is beyond the scope of the present analysis.

---

<sup>2</sup>Alternatively, we recall that in the hot settling flow  $H/R \sim 1$  and  $H/R \simeq c_s/v_{\text{ff}} \simeq c_s/(\sqrt{2}\Omega_K R)$ . Then  $\tau_{\text{cond}}$  readily follows from equation (82).

## 7.2 Observable properties

### 7.2.1 Spin-Up/Spin-Down of the Neutron Star

The rate of spin-up of the accreting NS is given by

$$\frac{d}{dt}(I_*\Omega) = \dot{J} - \dot{M}\Omega(R_*)R_*^2 \simeq -43s^3\alpha^2\dot{M}_{\text{Edd}}\Omega_K(R_*)R_*^2, \quad (92)$$

where  $I_*$  is the moment of inertia of the NS. We have made use of the fact that  $|\dot{J}| \gg |\dot{M}\Omega(R_*)R_*^2|$  for the self-similar solution, and used equation (19) for  $\dot{J}$ . The negative sign in the final expression implies that the accretion flow spins down the star. The above equation is for an unmagnetized NS. If the NS has a magnetosphere, the inner edge of the accretion flow is at the magnetospheric radius,  $R_m$ . In this case, let us define  $s$  by  $\Omega_* = s\Omega_K(R_m) = s\Omega_K(R_*)(R_m/R_*)^{-3/2}$ . Substituting this in equation (92) with  $I_* = \text{constant}$  and integrating, we obtain

$$s = \frac{s_0}{\sqrt{1+t/\tau}}, \quad \tau = \frac{I_*}{86s_0^2\alpha^2\dot{M}_{\text{Edd}}R_*^2} \left(\frac{R_m}{R_*}\right)^{-3/2}, \quad (93)$$

where  $s_0 = s(t=0)$ . The same result is valid for an unmagnetized NS by setting  $R_m = R_*$ . The quantity  $\tau$  is the characteristic spin-down time of the NS. For a spherical NS of constant density,  $I_* = 2M_*R_*^2/5 = (0.8 \times 10^{33} \text{ g})mR_*^2$ . Substituting this expression, we obtain the spin-down rate  $\dot{P}_*/P_* = \tau^{-1}$  with

$$\tau \simeq 6.7 \times 10^{12} s^{-2} \alpha^{-2} \left(\frac{R_m}{R_*}\right)^{-3/2} \quad s = 2 \times 10^8 s_{0.1}^{-2} \alpha_{0.1}^{-2} \left(\frac{R_m}{R_*}\right)^{-3/2} \text{ yr}. \quad (94)$$

Note the remarkable fact that the spin-down time scale is independent of the mass of the NS, and the mass accretion rate! For the magnetic case, the rate depends on the radius ratio  $R_m/R_*$ .

It is customary to express the spin-down rate as  $\dot{P}_*/P_*^2$ . Writing

$$P_* = \frac{2\pi}{s\Omega_K(R_*)} \left(\frac{R_m}{R_*}\right)^{3/2} \quad (95)$$

and  $\Omega_K(R_*) \simeq 10^4 m_{1.4}^{-1} \text{ rad/s}$ , where  $R_* = 3R_g$  and  $m_{1.4} = M_*/(1.4M_{\text{Sun}})$ , we obtain

$$\frac{\dot{P}_*}{P_*^2} \simeq 2.4 \times 10^{-10} m_{1.4}^{-1} \alpha^2 s^3 \text{ s}^{-2} = 2.7 \times 10^{-12} m_{1.4}^{-1} \alpha_{0.3}^2 s_{0.5}^3 \text{ s}^{-2}, \quad (96)$$

where  $s_{0.5} = s/0.5$ . This spin-down rate is in good agreement with observational data on the spin-down of X-ray pulsars for which Yi, Wheeler & Vishniac (1997) invoked ADAFs: 4U 1626-67 has  $\dot{P}/P^2 \approx 8 \times 10^{-13} \text{ s}^{-2}$  and  $P = 7.7 \text{ s}$ ; OAO 1657-415 has  $\dot{P}/P^2 \approx 2 \times 10^{-12} \text{ s}^{-2}$  and  $P = 38 \text{ s}$ , and GX 1+4 has  $\dot{P}/P^2 \approx 3.7 \times 10^{-12} \text{ s}^{-2}$  and  $P = 122 \text{ s}$ . Since the spin-down rate is quite sensitive to  $\alpha$  and  $s$ , the observed data in individual systems can be fitted by small adjustment of these parameters.

### 7.2.2 Luminosity

In computing the luminosity of the accretion flow, we must allow for the energy release in both the boundary layer and the self-similar settling zone. We calculate their luminosities separately.

Radiation from the self-similar hot brake flow may be calculated following the methods described by Popham & Narayan (1995) for a thin disk. This method assumes that the luminosity at a given radius is determined by the local viscous energy production. This is a legitimate approximation for the settling flow in which  $q^- = q^+$ . Keeping only the dominant terms, we find

$$L_{SS} = \frac{GM_* \dot{M}}{R_{in}} (1 - js) + \dot{M} \int_{P_{in}}^{P_{out}} \frac{dP}{\rho}, \quad (97)$$

where  $R_{in} = R_* + \Delta_{BL}$  is the inner radius of the self-similar zone and  $\Delta_{BL} \ll R_*$  is the thickness of the boundary layer. Here the first term inside the parentheses represents the luminosity associated with the potential energy of the infalling gas,  $L_{\text{pot}}$ , the second term  $-js$  is the luminosity associated with the rotational energy extracted from the star,  $L_{\text{rot}}$  (note,  $j < 0$  in the self-similar solution), and the final integral is the “enthalpy correction”,  $L_{\text{enth}}$ . Using the analytical solution (21)–(24) and assuming  $p_{\text{out}} = 0$  for simplicity, we obtain

$$L_{\text{pot}} = \dot{M}_{\text{Edd}} c^2 \frac{\dot{m}}{2r_*}, \quad (98)$$

$$L_{\text{rot}} = 43 \dot{M}_{\text{Edd}} c^2 \frac{\alpha^2}{2r_*} s^4, \quad (99)$$

$$L_{\text{enth}} = -\dot{M}_{\text{Edd}} c^2 \frac{\dot{m}}{2r_*}. \quad (100)$$

Note that the leading terms in  $L_{\text{pot}}$  and  $L_{\text{enth}}$  cancel each other exactly. The

luminosity of the self-similar flow is thus

$$L_{SS} \simeq 6.2 \times 10^{34} m r_3^{-1} \dot{m}_{-2} s_{0.1}^2 + 8.9 \times 10^{33} m r_3^{-1} \alpha_{0.1}^2 s_{0.1}^4 \text{ erg s}^{-1}, \quad (101)$$

where  $\dot{m}_{-2} = \dot{m}/0.01$ ,  $s_{0.1} = s/0.1$ ,  $r_3 = r_*/3$ , and we have assumed  $s \ll 1$ . Note that luminosity not associated with dissipation of rotational energy, represented by the first term in equation (101), is much less than the commonly assumed  $\sim GM_* \dot{M}/R_*$ . This is because the negative enthalpy term has a large magnitude, as a result of the fact that the settling flow is akin to a pressure supported, quasi-stationary atmosphere.

The second term in equation (101) is the luminosity of the settling zone. Since the self-similar solution for this zone is independent of  $\dot{m}$ , the luminosity too shows no  $\dot{m}$  dependence. Indeed, the luminosity remains finite even as  $\dot{m} \rightarrow 0$ . How is this possible, and where does the energy come from? The answer is that the luminosity of the settling zone is supplied by the central star. As the star spins down, it does work on the accretion flow and the energy released comes out as bremsstrahlung radiation.

The boundary layer luminosity requires a different method of calculation since viscous energy production is negligible in this zone:  $\Omega \simeq \text{constant}$ , and so  $q^+ \propto (d\Omega/dR)^2 \simeq 0$ . As the accreting gas cools in the boundary layer, starting from a nearly virial temperature  $\sim 10^{12}$  K on the outside down to the NS temperature  $\sim 10^7$  K near the surface, the thermal energy in the gas is emitted as radiation. To estimate the luminosity, we use the energy balance equation, which is the sum of equations (4),(5):

$$-q^- = \frac{\rho v}{\gamma - 1} \frac{dc_s^2}{dR} - v c_s^2 \frac{d\rho}{dR} = \frac{\gamma}{\gamma - 1} \rho v \frac{dc_s^2}{dR} - v \frac{dP}{dR}. \quad (102)$$

We can neglect the  $dp/dR$  term because the pressure  $p$  is essentially constant in the boundary layer. To obtain the luminosity we integrate over the boundary layer

$$L_{BL} = \int q^- 4\pi R^2 dR = - \int \frac{\gamma}{\gamma - 1} 4\pi R^2 \rho v \frac{dc_s^2}{dR} dR = \frac{\gamma}{\gamma - 1} \dot{M} (\Delta c_s^2). \quad (103)$$

Since  $c_s^2$  starts from nearly virial value and reaches close to zero,  $\Delta c_s^2 \simeq GM_*/R_*$ . More precisely,  $\Delta c_s^2 = c^2 \Delta(\theta_p + \theta_e) \simeq c^2 \theta_{p0} r_*^{-1}$ . Therefore, the boundary layer luminosity is

$$L_{BL} = \frac{\gamma}{\gamma - 1} \dot{M}_{\text{Edd}} c^2 \frac{\dot{m}}{6r_*} \approx 1.7 \times 10^{36} m \dot{m}_{-2} r_3^{-1}, \quad (104)$$

where we have assumed  $\gamma = 5/3$ . The total luminosity of the system is  $L = L_{SS} + L_{BL}$ . Note that  $L_{BL}$  has the same scaling as the first term in  $L_{SS}$  [Eq. (101)] and dominates the latter unless  $s \rightarrow 1$ .

### 7.2.3 Effect of Comptonization

Using the self-similar solution (21),(24), we may readily estimate the electron scattering optical depth and the  $y$ -parameter.<sup>3</sup> The optical depth is

$$\tau_{es} \simeq \rho \kappa_{es} R \simeq 10^3 \alpha s^2 r^{-1} \sim \alpha_{0.1} s_{0.1}^2 r^{-1}, \quad (105)$$

where  $\kappa_{es} = \sigma_T/m_p$  is the electron scattering opacity for ionized hydrogen. Since  $r \geq 3$ , we see that  $\tau_{es} \leq 1/3$  for reasonable parameters and the radiation is optically thin to electron scattering. The  $y$ -parameter is

$$y = 16\theta_e^2 \tau_{es} \simeq 2 \times 10^6 \alpha s^2 r^{-2} \sim 2 \times 10^3 \alpha_{0.1} s_{0.1}^2 r^{-2}. \quad (106)$$

The radius at which  $y \sim 1$  is

$$r_c \sim 45 \alpha_{0.1}^{1/2} s_{0.1}. \quad (107)$$

Above this radius the inverse Compton scattering is small and the self-similar solution is valid. For  $r < r_c$ , however, Comptonization is important and the electron temperature profile will be modified from the self-similar form. Since the electron-proton collisions are relatively weak (the plasma is two-temperature), other quantities, e.g., the density, proton temperature, etc., are unaffected. Comptonization is unimportant for low-viscosity flows,  $\alpha \lesssim 0.01$  around slowly rotating NSs,  $s \lesssim 0.01$ , because then  $r_c < r_*$ .

### 7.2.4 Spectrum

We now estimate the spectrum of radiation emitted from the hot brake accretion flow. Let us neglect inverse Compton scattering for the moment. The relativistic bremsstrahlung emissivity is approximated as

$$\epsilon_\nu \propto \rho^2 \exp(-(h\nu/kT_e)) \text{ erg cm}^{-3} \text{ s}^{-1} \text{ Hz}^{-1}. \quad (108)$$

---

<sup>3</sup>Here we just estimate where the effect of Comptonization becomes significant. For better analytical approximations see, for instance, Dermer, Liang & Canfield (1991); Titarchuk & Lyubarskij (1995). (In the latter paper, the expression for  $y$  is not given, but it can be inferred using equation [24]:  $y = \tau_{es}[(\alpha + 3)\theta/(1 + \theta) + 4d_0^{1/\alpha}\theta^2]$ .) Comptonization of free-free radiation has also been considered by Titarchuk (1989).



Therefore the luminosity per unit frequency is

$$L_\nu \propto \int_{R_*}^{\infty} \rho^2 e^{-h\nu/kT_e} 2\pi R^2 dR \propto \int_{1/\nu_m}^{\infty} t^{-3} e^{-\nu t} dt \propto \nu^2 \Gamma(-2, \nu/\nu_m), \quad (109)$$

where  $\Gamma(a, z) = \int_z^{\infty} t^{a-1} e^{-t} dt$  is the incomplete gamma-function and  $\nu_m = kT_e(R_*)/h$  is the maximum frequency. Above  $\nu_m$  the spectrum falls exponentially and below  $\nu_m$  it is nearly flat. We may, thus, replace the exponential in the integral with a square function which is equal to unity for  $\nu < \nu_m$  and 0 for  $\nu > \nu_m$ . With this approximation

$$L_\nu \simeq \frac{3}{2} \frac{L_{SS}}{\nu_m} \left( 1 - \frac{\nu^2}{\nu_m^2} \right), \quad (110)$$

where  $L_{SS} = \int L_\nu d\nu$  is the total luminosity of the self-similar flow, represented by equation (101). The break frequency,  $\nu_m$ , is roughly given by  $h\nu_m \sim 2.7$  MeV for a typical electron temperature  $T_{e,\max} \sim 10^{10.5}$  °K [cf., equation (24)]. At a typical x-ray energy,  $h\nu \sim 3$  keV, the observed luminosity per decade is

$$\nu L_\nu \simeq 1.7 \times 10^{31} m \alpha_{0.1}^2 s_{0.1}^4 \left( \frac{h\nu}{3 \text{ keV}} \right) \text{ erg s}^{-1}, \quad (111)$$

i.e.,  $\nu L_\nu \sim 1.5 \times 10^{32}$  for a 300 Hz neutron star ( $s_{0.1} \sim 1.6$ ). The spectrum is very hard with a photon index of order unity. Therefore, the luminosity per decade is much greater at higher photon energies and may be as high as  $\sim \text{few} \times 10^{34} - 10^{35}$  erg/s at  $h\nu \sim \text{MeV}$ .

As shown in the previous section, Comptonization becomes important below the radius  $r_c$ . At  $r_c$ ,  $y \approx 1$  and the electron temperature is

$$T_e(r_c) \sim 2.7 \text{ MeV} / \sqrt{r_c} \sim 400 \alpha_{0.1}^{-1/4} s_{0.1}^{-1/2} \text{ keV}. \quad (112)$$

For  $r < r_c$ , the electron temperature will be determined self-consistently by Compton cooling rather than by bremsstrahlung emission. Computing the spectrum from this region is beyond the scope of the paper. We also do not attempt to calculate the spectrum of the radiation from the boundary layer.

## 8 Conclusions

In this paper we present the analytical self-similar solution describing this *hot brake flow*. The hot brake flow exists at accretion rates as low as a few

percent of Eddington or smaller. We studied its properties and showed that it is stable with respect to winds/outflows and convection, as well as thermally stable (when the effects of thermal conduction are self-consistently included). The flow is subsonic everywhere. The flow is cooling-dominated, it is powered by the rotational energy of the central accretor which is braked by viscous torques. A very interesting property of the flow is that, except for the inflow velocity, all gas properties, such as density, temperature, angular velocity, luminosity, and angular momentum flux, are independent of the mass accretion rate (the flow properties do depend on the NS spin). This property implies that the density, temperature and angular velocity of the gas at any radius are completely independent of the outer boundary conditions. Therefore, such a flow cannot be matched to a general external medium. Hence, there is a “transition region”, represented by another self-similar solution, which has an extra degree of freedom which permits the hot accretion flow to match general outer boundary conditions. Matching the hot flow on the inside to general boundary conditions at the star surface occurs via another transition region, known as the “boundary layer”. A self-similar solution representing the boundary layer has also been derived.

Although we presented the hot break solution in the context of a neutron star, a similar accretion flow will certainly occur around a rapidly spinning white dwarf, and even around a spinning black hole, provided the Blandford & Znajek (1977) mechanism is efficient enough to power the MHD hot brake flow (Medvedev & Menou 2002; Perna, et al. 2003; Medvedev & Murray 2002).

## References

- Abramowicz, M. A., Chen, X., Kato, S., Lasota, J.-P., & Regev, O. 1995, *ApJ*, 438, L37
- Abramowicz, M. A., Czerny, B., Lasota, J. P., & Szuszkiewicz, E. 1988, *ApJ*, 332, 646
- Abramowicz, M. A., Lasota, J.-P., & Igumenshchev, I. V. 2000, *MNRAS*, 314, 775
- Alme, M. L., & Wilson, J. R. 1973, *ApJ*, 186, 1015
- Ball, G. H., Narayan, R., & Quataert, E. 2001, *ApJ*, 552, 221

- Blandford, R. D., & Begelman, M. C. 1999, *MNRAS*, 303, L1
- Blandford, R. D., & Znajek, R. L. 1977, *MNRAS*, 179, 433
- Chakrabarti, S. K., & Sahu, S. A. 1997, *ApJ*, 323, 382
- Chandran, B. D. G., & Cowley, S. C. 1998, *PRL*, 80, 3077
- Chen, X., Abramowicz, M. A., & Lasota, J.-P. 1997, *ApJ*, 476, 61
- Cowie, L. L., & McKee, C. F. 1977, *ApJ*, 211, 135
- Dermer, C. D., Liang, E. P., & Canfield, E. 1991, *ApJ* 369, 410
- Deufel, B., Dullemond, C. P., & Spruit, H. C. 2001, *A&A*, 377, 955
- Davies, R. E., & Pringle, J. E. 1981, *MNRAS*, 196, 209
- Field, G. B. 1965, *ApJ*, 142, 531
- Goldreich, P., & Lynden-Bell, D. 1965, *MNRAS*, 130, 125
- Goldreich, P., & Tremaine, S. 1978, *ApJ*, 222, 850
- Ichimaru, S. 1977, *ApJ*, 214, 840
- Igumenshchev, I. V. & Abramowicz, M. A. 1999, *MNRAS*, 303, 309
- Igumenshchev, I. V., & Abramowicz, M. A. 2000, *ApJS*, 130, 463
- Ikhsanov, N. R. 2001, *A&A*, 367, 549
- Ikhsanov, N. R. 2003, *A&A*, 399, 1147
- Julian, W. H., & Toomre, A. 1966, *ApJ*, 146, 810
- Kato, S., Abramowicz, M. A., & Chen, X. 1996, *Proc. R. Soc. Japan*, 48, 67
- Kato, S., Yamasaki, T., Abramowicz, M. A., & Chen, X. 1997, *Proc. R. Soc. Japan*, 49, 221
- Kluźniak, W., & Wilson, J. R. 1991, *ApJ*, 372, L87
- Kylafis, N.D., & Lamb, D.Q. 1982, *ApJ*, 48, 239

- Mal'ushkin, L., & Kulsrud, R. 2001, *ApJ*, 549, 402
- Mal'ushkin, L. 2000, *ApJ*, 554, 561
- Medvedev, M. V., & Menou, K. 2002, *ApJ*, 565, L39
- Medvedev, M. V., & Murray, N. 2002, *ApJ*, 581, 431
- Medvedev, M. V., & Narayan, R. 2001a, *ApJ*, 554, 1255
- Medvedev, M. V., & Narayan, R. 2001b, astro-ph/0107066
- Narayan, R., Igumenshchev, I. V., & Abramowicz, M. A. 2000, *ApJ*, 539, 798
- Narayan, R., Kato, S., & Honma, F. 1997, *ApJ*, 476, 49
- Narayan, R., Mahadevan, R., & Quataert, E. 1997, in *Theory of Black Hole Accretion Discs*, ed M. A. Abramowicz, G. Bjornsson, J. E. Pringle, Cambridge Univ. Press, p148
- Narayan, R., & Medvedev, M. V. 2003, *MNRAS*, 343, 1007
- Narayan, R., Kato, S., & Honma, F. 1997, *ApJ*, 476, 49
- Narayan, R., & Popham, R. 1993, *Nature*, 362, 820
- Narayan, R., & Yi, I. 1994, *ApJ*, 428, L13
- Narayan, R., & Yi, I. 1995, *ApJ*, 444, 231
- Narayan, R., & Yi, I. 1995, *ApJ*, 452, 710
- Paczynski, B. 1991, *ApJ*, 370, 597
- Paczynski, B., & Wiita, P. J. 1980, *A&A*, 88, 23
- Perna, R., McDowell, J., Menou, K., Raymond, J., & Medvedev, M. V. 2003, *ApJ*, 598, 545
- Popham, R., & Narayan, R. 1995, *ApJ*, 442, 337
- Popham, R., & Narayan, R. 1992, *ApJ*, 394, 255

- Popham, R., & Sunyaev, R. 2001, *ApJ*, 547, 355
- Piran, T. 1978, *ApJ*, 221, 652
- Pringle, J. E. 1977, *MNRAS*, 178, 195
- Quataert, E., & Gruzinov, A. 2000, *ApJ*, 539, 809
- Rechester, A. B., & Rosenbluth, M. N. 1978, *PRL*, 40, 38
- Rees, M. J., Phinney, E. S., Begelman, M. C., & Blandford, R. D. 1982, *Nature*, 295, 17
- Shakura, N. I. & Sunyaev, R. A. 1976, *MNRAS*, 175, 613
- Shapiro, S. L., Lightman, A. P., & Eardley D. M. 1976, *ApJ*, 204, 187
- Shapiro, S. L., & Salpeter, E. E. 1975, *ApJ*, 198, 671
- Spitzer, L. 1962, *Physics of fully ionized gases* (New York: Interscience)
- Titarchuk, L. 1989, *Astrophysics* (tr. Astrofizika), 29, 63
- Titarchuk, L., Lapidus, I., & Muslimov, A. 1998, *ApJ*, 499, 315
- Titarchuk, L. & Lyubarskij, Yu. 1995, *ApJ*, 450, 876
- Titarchuk, L. & Osherovich, V. 1999, *ApJ*, 518, L95
- Toomre, A. 1977, *ARA&A*, 15, 437
- Turolla, R., Zampieri, L., Colpi, M., & Treves, A. 1994, *ApJ*, 426, L35
- Wandel, A., & Liang, E. P. 1991, *ApJ*, 380, 84
- Yi, I., Wheeler, J. C., & Vishniac, E. 1997, *ApJ*, 481, L51
- Zampieri, L., Turolla, R., Zane, S., & Treves, A. 1995, *ApJ*, 439, 849
- Zane, S., Turolla, R., & Treves, A. 1998, *ApJ*, 501, 258
- Zeldovich, Y. B., & Shakura, N. I. 1969, *Soviet Astron.–AJ*, 13, 175